Journal of Basrah Researches ((Sciences)) Vol. (45). No. 2 (2019)

Available online at:
https://www.iasj.net/iasj?func=issueTOC&isId=9923&uiLanguage=ar

ISSN .1817 .2695

Received 5-9-2019, Accepted 11-11-2019

STUDY OF PETROPHYSICAL PROPERTIES OF MISHRIF AND YAMAMA FORMATIONS AT SELECTED FIELDS, SOUTH IRAQ

[1]AMNA M. HANDHAL [2]HUSSEIN A. CHAFEET [3]NAWFAL A. DAHHAM AND [4]RAGHAD BASHER

[1, 4] Department of Geology, Collage of Science, University of Basrah, Basrah, Iraq

[2, 3] Department of Oil and Gas Engineering, College of Oil and Gas Engineering, Basrah University for Oil and Gas, Basrah, Iraq

Email: [1]amhgeo@gmail.com, [2]hussein.aliwi@buog.edu.iq, [3]Nawfal.adnan@buog.edu.iq

ABSTRACT

The characteristics of reservoir require reliable knowledge of certain fundamental reservoir properties. Log measurements can define or at least infer these properties: resistivity, porosity, shale volume, lithology, water saturation, hydrocarbon saturation and permeability. The current study represents evaluation of petrophysical properties in wells Fa-1, Fa-2 and Fa-3 in Faiha oilfield and in well Snd-2 in Sindibad oilfield of Mishrif and Yamama formations, southern Iraq.

The petrophysical evaluation was based on well logs data to delineate the reservoir characteristics of Mishrif and Yamama formations. The available well logs such as (Gamma ray, SP, Resistivity (MSF, ILL), Sonic, Density and Neutron logs) are digitized using Didger software (v.4). The environmental corrections and petrophysical parameters such as porosity, water saturation, hydrocarbon saturation and shale volume were computed and interpreted using Interactive Petrophysics software (IP). Petrophysical properties were determined and plotted as computer processing interpretation (CPI) using Interactive Petrophysics software. Lithological study of Mishrif Formation appears that it consists mainly of interbedded limestone, dolomite and shale, whereas lithological study of Yamama Formation appears that it consists mainly of interbedded limestone, dolomite and shale in some depths.

Interpretations of well logs of Mishrif Formation in well Snd-2 it have good hydrocarbon saturation. Results also referred that hydrocarbon saturation and permeability in some ranges of the formation especially in MB unit is very high, in addition to the low movable oil and this may indication of the heavy oil in the formation. While interpretations of well logs of Yamama Formation in well Fa-1 indicated high hydrocarbon saturation. In general, the reservoir characteristics of Yamama Formation in Fa-1 are better than wells Fa-2 and Snd-2, and reservoir characteristics of Mishrif Formation in well Snd-2 better than Fa-1 and Fa-3 according to petrophysical properties and hydrocarbon saturation. Mishrif Formation in Faiha oilfield is divided into nine zones and nine zones in Sindibad oilfield, while Yamama Formation is divided into six zones in Faiha oilfield and seven zones in Sindibad oilfield according to Behavior of well logs and Shale volume.

Keywords: Petrophysical Properties, Mishrif Formation, Yamama Formation, South Iraq, Well Logs.

1. INTRODUCTION

The Faiha and Sindibad Oil Fields consist of different reservoir zones and the zones considered for this study is Mishrif and Yamama formations. Petrophysical properties are the study of rock properties and their interactions with fluids (gases, liquid hydrocarbons and aqueous solutions). Well logging is the technique of making petrophysical measurements in the subsurface earth formations through the drilled borehole in order to determine both the physical and chemical properties of rocks and the fluid they contain [1]. The objective is to locate, define, and produce hydrocarbons from a given reservoir and it is also known as formation evaluation. Due to the enormous amount of data well logging can provide, the technology plays a pivotal role in hydrocarbon exploration and production industry. These techniques can be used in all phases of hydrocarbon exploration and production process. Rapid and sophisticated development in well logging technology has revolutionized the hydrocarbon industry [2]. Moreover, it can use a group of logs for many wells to describe the structural, stratigraphy, facies relationships for the deposition environments and reservoir engineering.

The main purpose of this study is to make use of all the available sets of well logs data acquired in the study area especially related to open wells from Fa-1, Fa-2 and Fa-3 in Faiha Oil Field and from wells Snd-1 and Snd-2 in Sindibad Oil Field to determine the petrophysical properties for each zone in Mishrif and Yamama formations, and therefore to evaluate the performance production of the reservoir. This study deals with pre-interpretation and the internal properties of Mishrif and Yamama formations. The study includes two steps, the pre-interpretation and the interpretation. The pre-interpretation includes the determination of effective porosity (corrected to shale effects) and all the parameters that are required in the interpretation processes. The interpretations were made using Interactive Petrophysics software v3.5 (interactive software to carry out interpretations and log corrections for borehole environment and invasion effects).

2. STUDY AREA

The Faiha and Sindibad oilfields are located in Basrah Governorate, southern Iraq. Faiha field is located within the area of exploration (Block-9). This structure is located in the southeastern part of Iraq, along Iraqi-Iranian borders, about (20 km.) towards northeastern of the Basrah city. It is bordered from the north Majnoon oilfield, from the south Sindibad field, from the west Nahr Bin Umr field. It covers an area of (2866 km.) which is a convex fold. The field lies approximately between the lines easting (215337.12-215502.00) m. and northing (3425691.05-3432610.00) m. as shown in Fig. (1). Sindibad field is located in the southeastern part at about (18 km.) of Basrah city and approximately (5 km.) of Iraqi-Iranian borders between the lines easting (785451-787500) m. and northing (3388161-3389000) m., (Basrah Oil Company). Many wells were drilled in Faiha Field (Fa-1, Fa-2 and Fa-3) and in Sindibad Field (Snd-1and Snd-2) to determine the Structural configuration and facies distribution of the reservoir rocks.

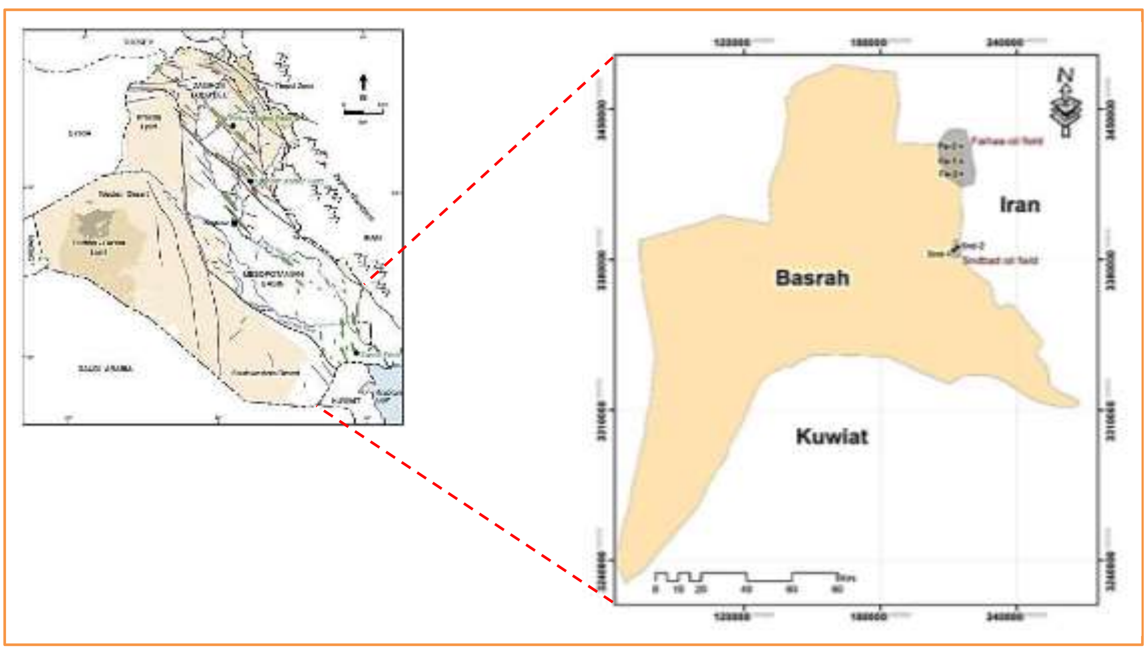

Figure 1: Location Map Of The Study Area.

3. METHODOLOGY

Using Interactive Petrophysics software v3.5 (IP) for analyze the geophysical well logs such as (Gamma Ray, Spontaneous Potential, Resistivity (MSF, ILL), Sonic, Density and Neutron logs) and plotted to evaluate the water and hydrocarbon saturations of Mishrif and Yamama formations using the Archie equation. The available open hole logs data were digitized in order to be imported into the appropriate software for analysis and interpretation, Didger (v.4) software was used in this very first step. The proper corrections (i.e. Shale effect, borehole conditions, depth of invasion, etc.) for Gamma ray, Resistivity, Density and Neutron logs, were applied before commencing the open hole well log analysis as based on Schlumberger's well log analysis basic corrections using Interactive Petrophysics software.

Calculate of shale volume (V_{sh}), petrophysical parameters such as porosities and use the NMR log to calculate the permeability.

Interactive Petrophysics software was used for well logs analysis and plotted to evaluate petrophysical properties as computer processing interpretation (CPI) of Mishrif and Yamama formations in Faiha and Sindibad fields.

4. PETROPHYSICAL PROPERTIES

For determining reservoir properties of Mishrif and Yamama formations, petrophysical parameters must be obtained and evaluated. These parameters include:

4.1 Calculation of Shale Volume (V_{sh})

Knowing the volume value of shale is very important due to that it affects directly on the different log tools. [3, 4] state that if there is any increase in the volume of shale in reservoir (10 % - 15 %), it has a noticeable impact and influence on porosity and water saturation calculated from logs. The volume of shale is calculated in many methods: calculated from Gamma ray, Spontaneous potential, Neutron and Resistivity Logs as follows: [5]

4.1.1 Resistivity log:

$$V_{sh}=\sqrt{\frac{Rsh}{Rt}} \qquad (1)$$

When: V_{sh}= Shale volume; R_{sh}= Resistivity of shale; R_t= True Resistivity [5]. This method is good in the following cases:

- Low porosity (Carbonate, Shale, Marl …etc.).
- Saturated formations with high hydrocarbon saturation.

4.1.2 Spontaneous potential log:

$$\mathbf{V_{sh}} = 1 - [SP - SP_{sh} / SP_{Cl} - SP_{sh}] \qquad (2)$$

When: SP= Spontaneous potential; $SP_{sh:}$ Spontaneous potential shale; $SP_{Cl:}$ Spontaneous potential clean. This method gives uncertain results in the following cases:

- Hydrocarbon-bearing formations (oil, gas), given high values for the (V_{sh}).

- Dispersed Clay [6].

4.1.3 Neutron log:

$\Phi_N = \Phi_e * \Phi_{NF} * V_{sh} * \Phi_{Nsh}$ (3)

When: Φ_N= Porosity is derived from Neutron log; Φ_e= Effective porosity; Φ_{NF}= Neutron porosity of fluid; Φ_{Nsh}= Neutron porosity for shale [5]. This method given good results in the following cases:

- Effective porosity few as in Shale, Marl …. etc. ($\Phi_e = \Phi_{NF} = 0$).

The equation becomes as follows:

$V_{sh} = \Phi_N / \Phi_{Nsh}$ (4)

- Give good results when the value of the Φ_{Nsh} high.

4.1.4 Gamma ray log:

To derive V_{sh} from gamma ray (GR Log), it is imperative that the gamma ray index (I_{GR}), determined by using equation of Schlumberger (1974) [7]

$I_{GR} = (GR_{log} - GR_{min})/(GR_{max} - GR_{min})$ (5)

When: I_{GR}= gamma ray index; GR_{log}= gamma ray reading of formation; GR_{min}= minimum gamma ray (clean sand or carbonate); GR_{max}= maximum gamma ray (shale). For the purpose of this work, the formula of Dresser Atlas (1979) [8] for older rocks was used to determine the shale volume.

$V_{sh} = 0.33 * [2 (2*IGR) - 1]$ (6)

In this study, the shale volume has been calculated by using (IP) program the results of calculating the volume of shale show an increase in volume more than (10%) in most deep intervals. Statistical analysis shows that the least percentage of shale was in Yamama Formation in well Fa-2 and the highest rate was in Yamama Formation in Fa-1. Besides that, layers boundaries have been determined and divide the formations into many zones based on behavior of logs and volume of shale. Mishrif Formation has been divided into nine zones in Faiha Field and nine zones in Sindibad Field, while Yamama Formation is divided into six zones in Faiha Field and seven zones in Sindibad Field as shown in Figures (2 to 13).

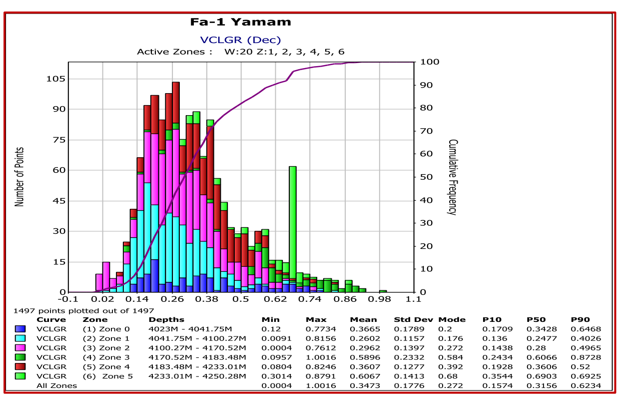

Figure 2: Statistical Analysis Of Shale Distribution For Yamama Formation In Fa-1.

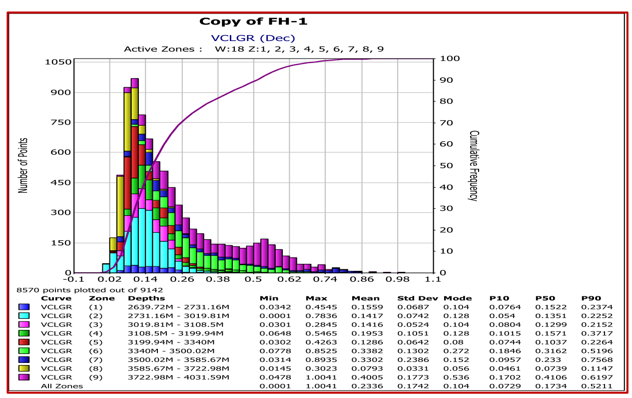

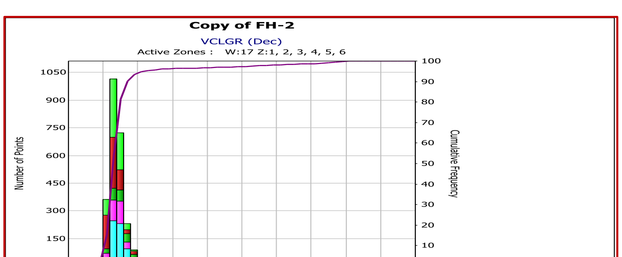

Figure 4: Statistical Analysis Of Shale Distribution For Yamama Formation In Fa-2.

Figure 3: Statistical Analysis Of Shale Distribution For Mishrif Formation In Fa-1.

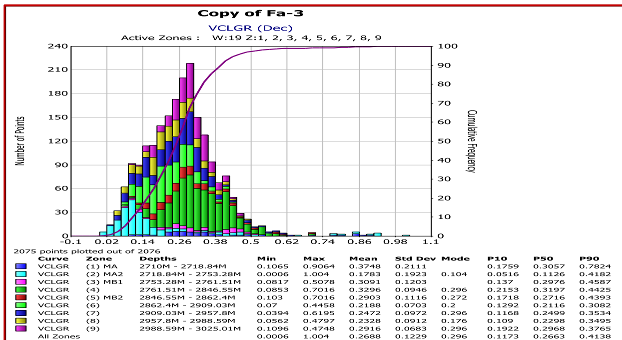

Curve	Zone	Depths	Min	Max	Mean	Std Dev	Mode	P10	P50	P90
VCLGR	(1) MA	2710M - 2718.84M	0.1065	0.9064	0.3748	0.2111		0.1759	0.3057	0.7824
VCLGR	(2) MA2	2718.84M - 2753.28M	0.0006	1.004	0.1783	0.1923	0.104	0.0516	0.1126	0.4182
VCLGR	(3) MB1	2753.28M - 2761.51M	0.0817	0.5078	0.3091	0.1203		0.137	0.2976	0.4587
VCLGR	(4)	2761.51M - 2846.55M	0.0853	0.7016	0.3296	0.0946	0.296	0.2153	0.3197	0.4425
VCLGR	(5) MB2	2846.55M - 2862.4M	0.103	0.7016	0.2903	0.1116	0.272	0.1718	0.2716	0.4393
VCLGR	(6)	2862.4M - 2909.03M	0.07	0.4458	0.2188	0.0703	0.2	0.1292	0.2116	0.3082
VCLGR	(7)	2909.03M - 2957.8M	0.0394	0.6195	0.2472	0.0972	0.296	0.1168	0.2499	0.3534
VCLGR	(8)	2957.8M - 2988.59M	0.0562	0.4797	0.2328	0.0912	0.176	0.109	0.2298	0.3495
VCLGR	(9)	2988.59M - 3025.01M	0.1096	0.4748	0.2916	0.0683	0.296	0.1922	0.2968	0.3765
All Zones			0.0006	1.004	0.2688	0.1229	0.296	0.1173	0.2663	0.4138

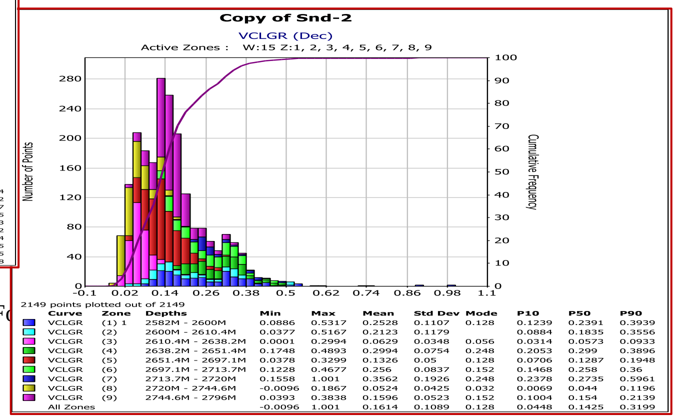

Curve	Zone	Depths	Min	Max	Mean	Std Dev	Mode	P10	P50	P90
VCLGR	(1) 1	2582M - 2600M	0.0886	0.5317	0.2528	0.1107	0.128	0.1239	0.2391	0.3939
VCLGR	(2)	2600M - 2610.4M	0.0377	0.5167	0.2123	0.1179		0.0884	0.1835	0.3556
VCLGR	(3)	2610.4M - 2638.2M	0.0001	0.2994	0.0629	0.0348	0.056	0.0314	0.0573	0.0933
VCLGR	(4)	2638.2M - 2651.4M	0.1748	0.4893	0.2994	0.0754	0.248	0.2053	0.299	0.3896
VCLGR	(5)	2651.4M - 2697.1M	0.0378	0.3299	0.1326	0.05	0.128	0.0706	0.1287	0.1948
VCLGR	(6)	2697.1M - 2713.7M	0.1228	0.4677	0.256	0.0837	0.152	0.1468	0.258	0.36
VCLGR	(7)	2713.7M - 2720M	0.1558	1.001	0.3562	0.1926	0.248	0.2378	0.2735	0.5961
VCLGR	(8)	2720M - 2744.6M	-0.0096	0.1867	0.0524	0.0425	0.032	0.0069	0.044	0.1196
VCLGR	(9)	2744.6M - 2796M	0.0393	0.3838	0.1596	0.0523	0.152	0.1004	0.154	0.2139
All Zones			-0.0096	1.001	0.1614	0.1089	0.128	0.0448	0.1425	0.3199

Figure 7: Statistical Analysis Of Shale Distribution For Mishrif Formation In Snd-2.

Figure 5: Statistical Analysis Of Shale Distribution Fo

Mishrif Formation In Fa-2

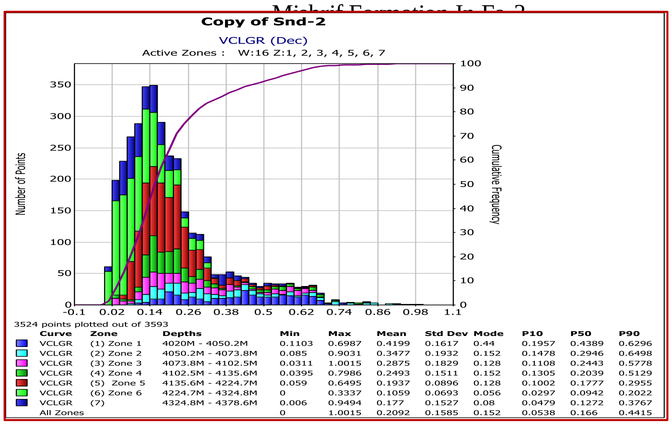

Curve	Zone	Depths	Min	Max	Mean	Std Dev	Mode	P10	P50	P90
VCLGR	(1) Zone 1	4020M - 4050.2M	0.1103	0.6987	0.4199	0.1617	0.44	0.1957	0.4389	0.6296
VCLGR	(2) Zone 2	4050.2M - 4073.8M	0.085	0.9031	0.3477	0.1932	0.152	0.1478	0.2946	0.6498
VCLGR	(3) Zone 3	4073.8M - 4102.5M	0.0311	1.0015	0.2875	0.1829	0.128	0.1108	0.2443	0.5778
VCLGR	(4) Zone 4	4102.5M - 4135.6M	0.0395	0.7986	0.2493	0.1511	0.152	0.1305	0.2039	0.5129
VCLGR	(5) Zone 5	4135.6M - 4224.7M	0.059	0.6495	0.1937	0.0896	0.128	0.1002	0.1777	0.2955
VCLGR	(6) Zone 6	4224.7M - 4324.8M	0	0.3337	0.1059	0.0693	0.056	0.0297	0.0942	0.2022
VCLGR	(7)	4324.8M - 4378.6M	0.006	0.9494	0.177	0.1527	0.08	0.0479	0.1272	0.3767
All Zones			0	1.0015	0.2092	0.1585	0.152	0.0538	0.166	0.4415

Figure 6: Statistical Analysis Of Shale Distribution For Yamama Formation In Snd-2.

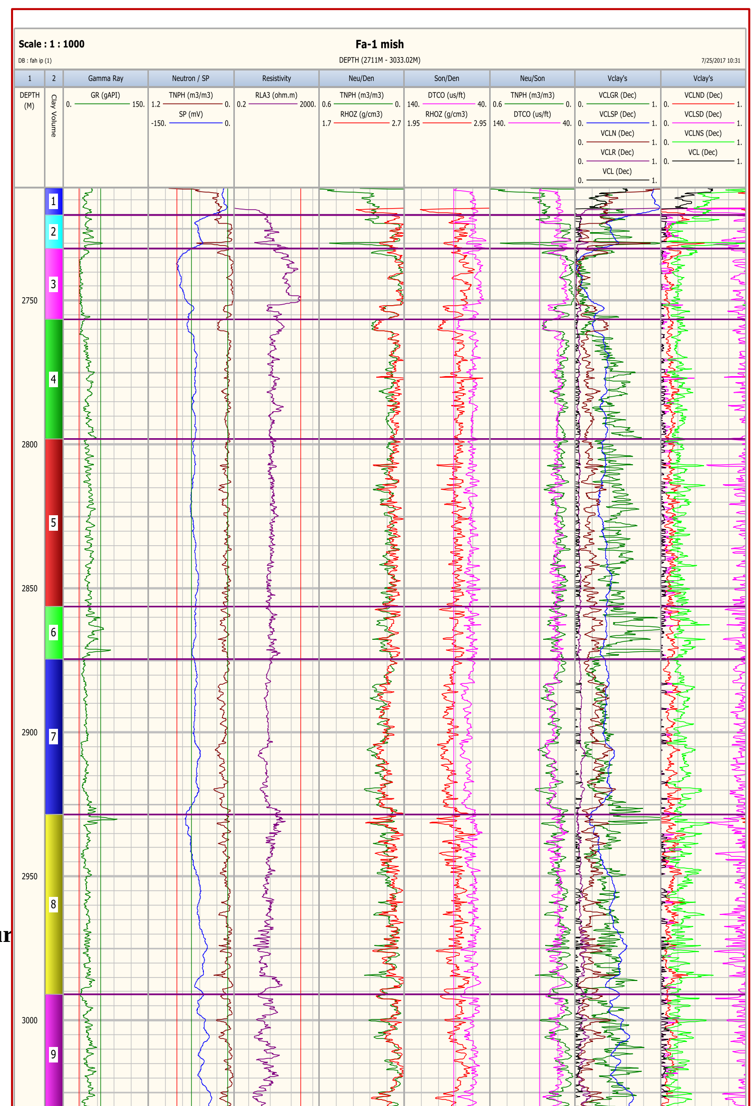

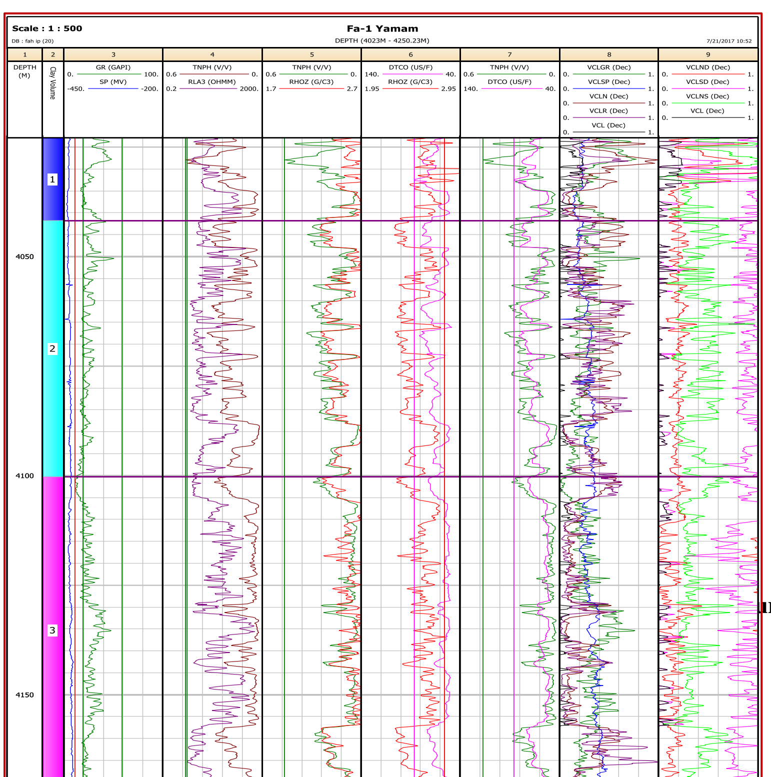

Figure 9: Shale Volume For Mishrif Formation In Fa-1.

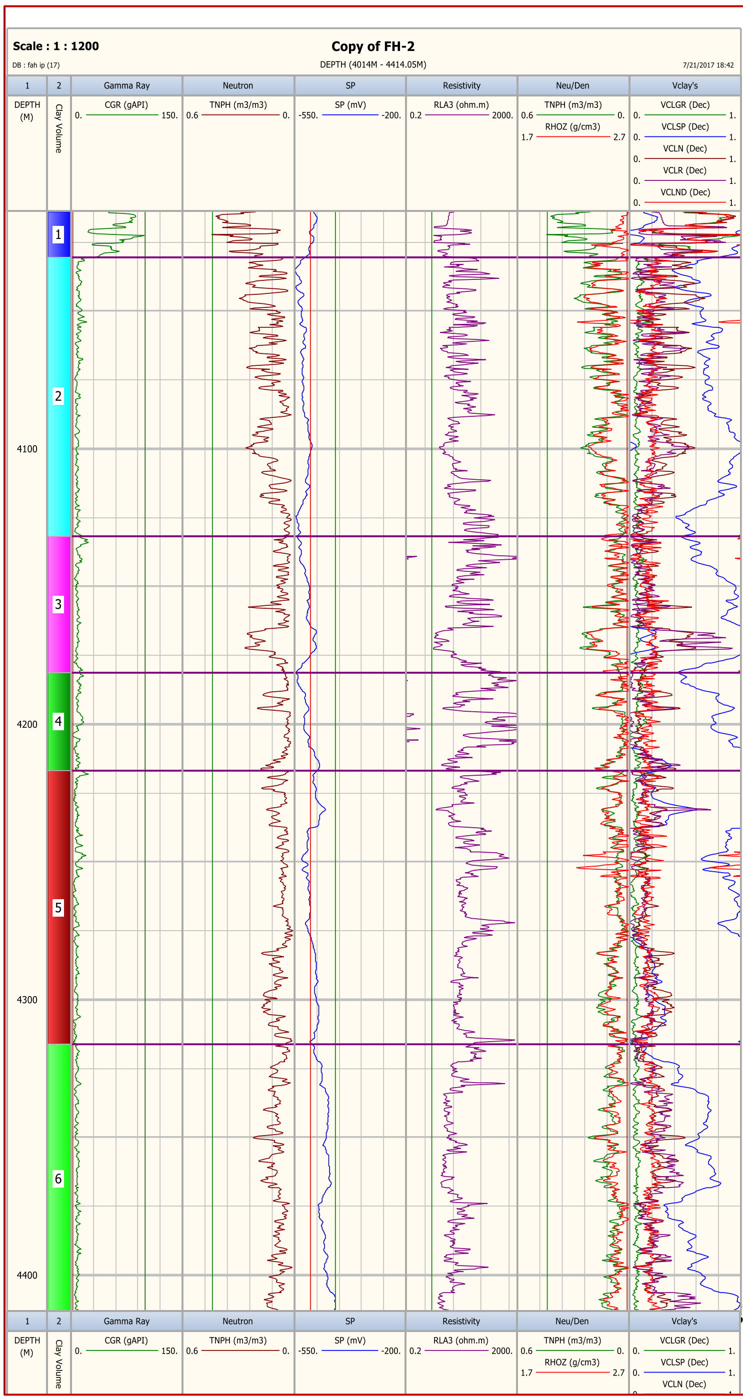

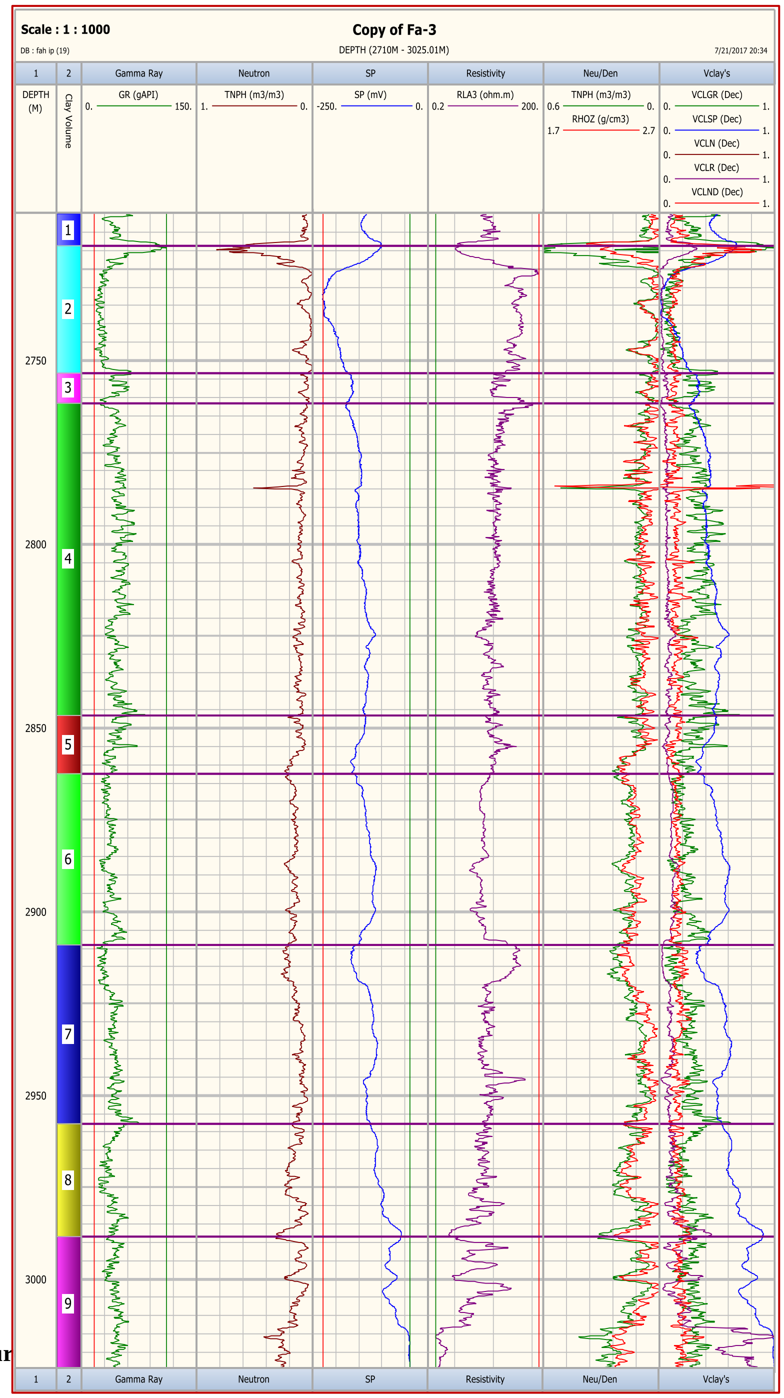

Figure 11: Shale Volume For Mishrif Formation In Fa-3.

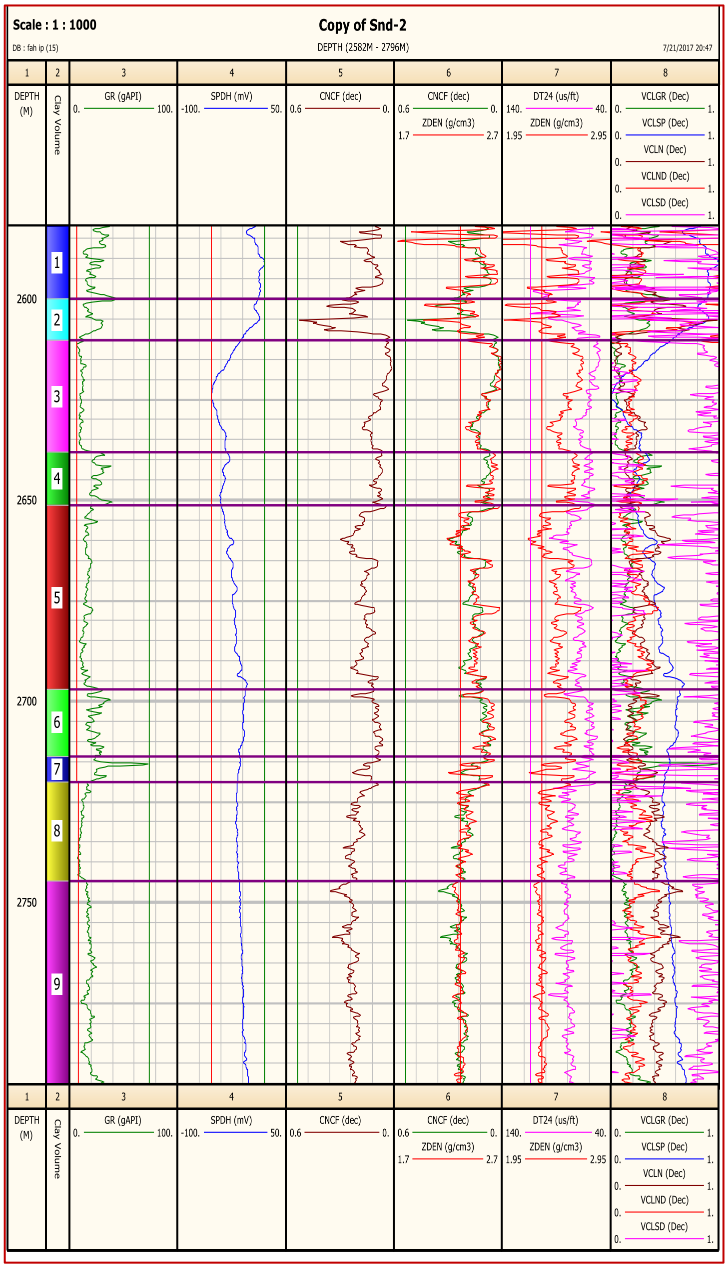

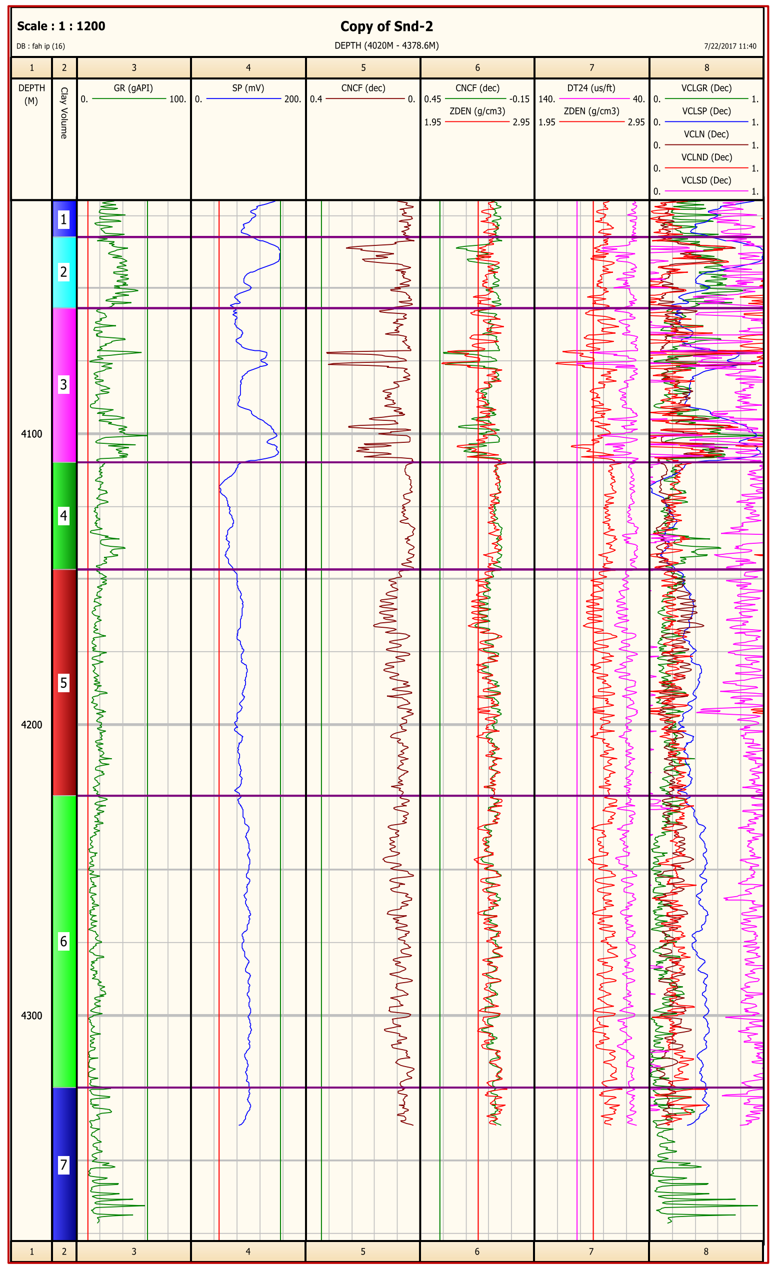

Figure 12: Shale Volume For Mishrif Formation In Snd-2.

Figure 13: Shale Volume For Yamama Formation In Snd-2.

4.2 Calculation of Formation Water Resistivity (Rw) from Sp. Log

The formation water resistivity is of great importance in studying of well records for it enters into the calculating of water saturation (Sw). There are several methods in calculating the formation water resistivity, such as direct measuring of typical sample of water formation or through (Cross Plot) the method of qualitative resistivity of formation water by applying the equation (Archie) in accordance with the water saturated layers.

Previously, getting the best values of (Rw) from (SP) log; provided that, the formation is clean of any shale deposit, porous, permeable, thick and saturated with water [9]. In current study this value has been calculated by (IP) program by using data entry of temperature degrees and Rmf (omh-m) then Rmf temperature and SP log to both Mishrif and Yamama formations.

4.3 Calculation of Total and Secondary Porosity

Total porosity within Yamama and Mishrif formations was determined from combination of Neutron - Density derived porosities. Neutron log measure the direct porosity after corrected based on the equation of Tiab & Donaldson (1996) [10].

$$Ø_{Ncorr.} = Ø_N - (V_{sh} * Ø_{Nsh}) \quad (7)$$

Where: $Ø_{Ncorr.}$= corrected porosity is derived from Neutron log for no clean rocks**;** $Ø_{Nsh}$= Neutron porosity for shale. Density porosity is derived from the bulk density of clean liquid filled formations when the matrix density (ρ_{ma}) and the density of the saturating fluids (ρ_f) are known, using Wyllie *et al.*, (1958) [11] equation:

$$Ø_D = (\rho_{ma} - \rho_b) / (\rho_{ma} - \rho_f) \quad (8)$$

Where: ρ_{ma}= density of matrix (2.71 gm/cm3 for limestone, 2.87 gm/cm3 for dolomite, 2.65 gm/cm3 for sandstone); ρ_f= density of fluid (1 gm/cm3 for fresh water, 1.1 gm/cm3 for saline water).

In intervals, whose shale volume is more than 10%, we used equation (9) to remove shale effect from porosity calculation:

$$Ø_{Dcorr.} = Ø_D - (V_{sh} * Ø_{Dsh}) \quad (9)$$

Where: $Ø_{Dcorr.}$= corrected porosity is derived from Density log for no clean rocks**;** $Ø_{Dsh}$= density porosity for shale.

Total porosity ($Ø_t$), whereas equation (10) is used in depths ($Ø_N < Ø_D$) and calculated as follows:

$$Ø_t = (Ø_N + Ø_D) / 2 \quad (10)$$

The effective porosity ($Ø_e$) is then calculated, using equation of Schlumberger (1998) [12] after total porosity corrected from shale volume:

$$Ø_e = Ø_t * (1-V_{sh}) \quad (11)$$

Sonic log (Δ_t) based on Wyllie time-average equation (12) was used to determine primary porosity:

$$Ø_S = (\Delta_{tlog} - \Delta_{tma}) / (\Delta_{tfl} - \Delta_{tma}) \quad (12)$$

Where: $Ø_S$= sonic derived porosity; Δ_{tlog}= interval transit time in the formation; Δ_{tma}= interval transit time in the matrix; Δ_{tfl}= interval transit time in the fluid in the formation.

Δ_t is increased due to the presence of hydrocarbon. To correct for hydrocarbon effect, [3] suggested the following empirical equations:

$$Ø = Ø_S * 0.7 \text{ (gas)} \quad (13)$$

$$Ø = Ø_S * 0.9 \text{ (oil)} \quad (14)$$

Then, in order to correct sonic porosity from shale effect within formation, the following equation is used:

$$Ø_{Scorr.} = Ø_S - (V_{sh} * Ø_{Ssh}) \quad (15)$$

Where: $Ø_{Scorr.}$= corrected sonic porosity; $Ø_S$= sonic derived porosity; $Ø_{Ssh}$= apparent porosity of the shale.

Secondary porosity index (SPI) was computed by the difference between total porosity and the primary porosity (that is determined from sonic log) after made corrections for shaliness and hydrocarbon effect:

$$SPI = (Ø_t - Ø_{Scorr.}) \quad (16)$$

Porosities of the Yamama and Mishrif formations have been calculated by using porosity logs, as shown in Figures (14 to 29), it has been observed that Yamama Formation has porosity values in Fa-1 better than Fa-2 and Snd-2. The total porosity of the formation was very effective and decrease in secondary porosity which is almost none in some depths. While the porosity of the Mishrif Formation in well Snd-2 was better than Fa-1 and Fa-3, it is from primary porosity type (effective) and secondary porosity is little or none in the formation.

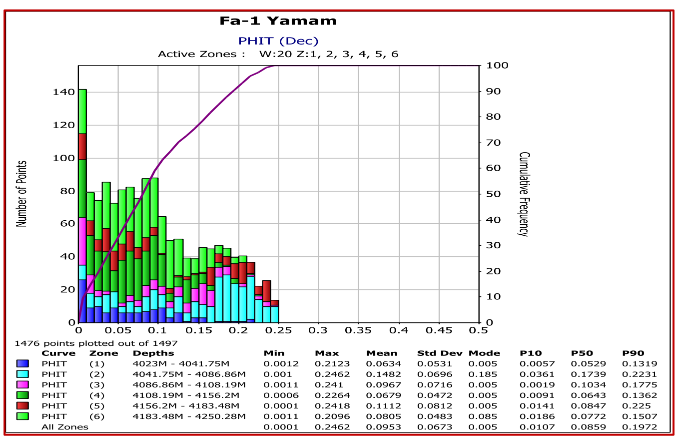

Figure 14: Total Porosity Values For Yamama Formation In Fa-1.

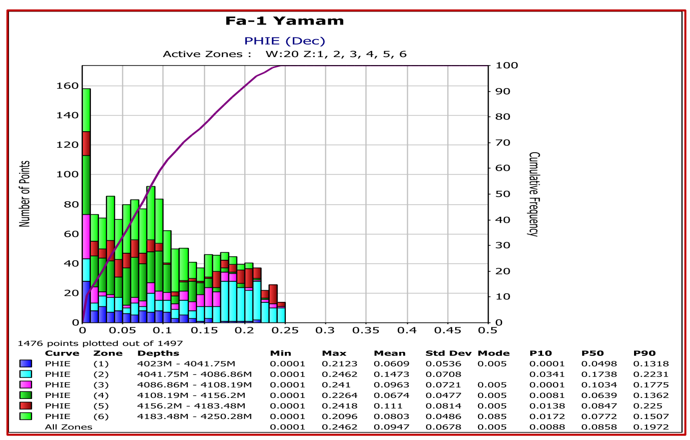

Figure 15: Effective Porosity Values For Yamama Formation In Fa-1.

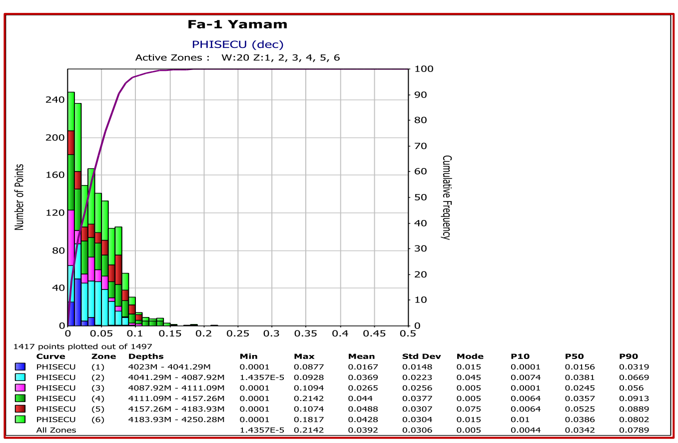

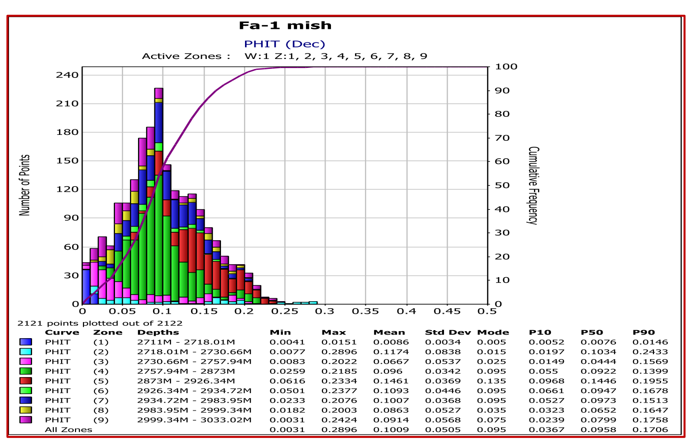

Figure 16: Secondary Porosity Values For Yamama Formation In Fa-1.

Figure 17: Total Porosity Values For Mishrif Formation In Fa-1.

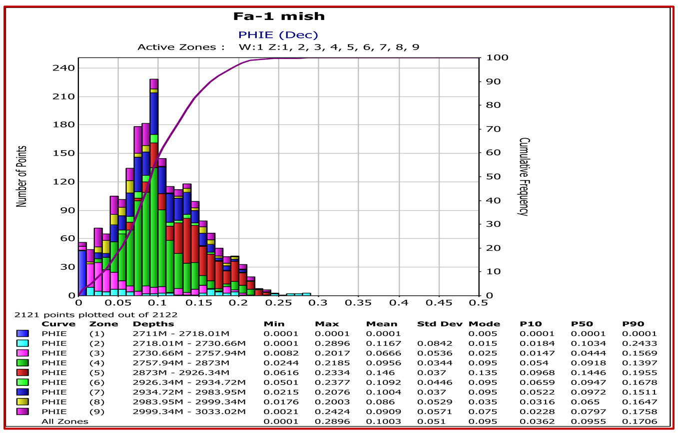

Figure 18: Effective Porosity Values For Mishrif Formation In Fa-1.

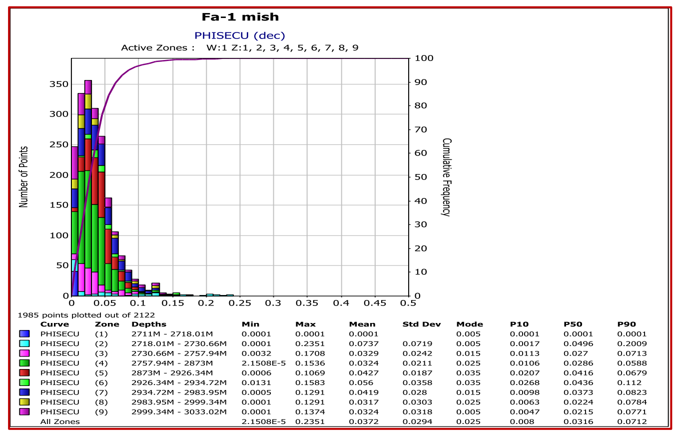

Figure 19: Secondary Porosity Values For Mishrif Formation In Fa-1.

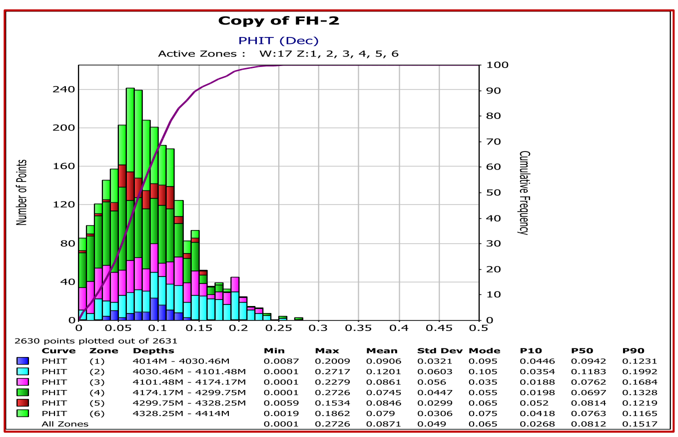

Figure 20: Total Porosity Values For Yamama Formation In Fa-2.

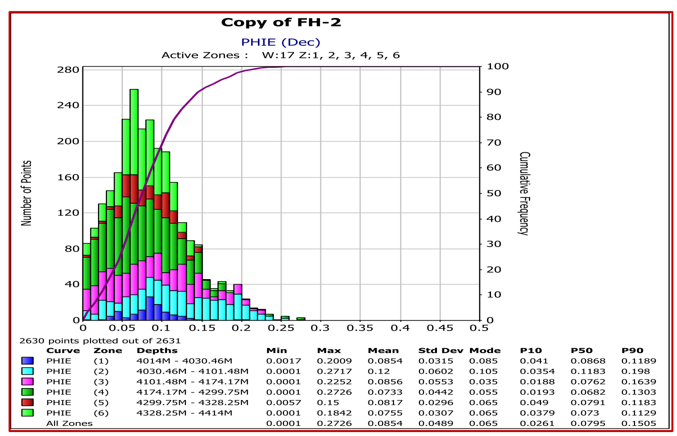

Figure 21: Effective Porosity Values For Yamama Formation In Fa-2.

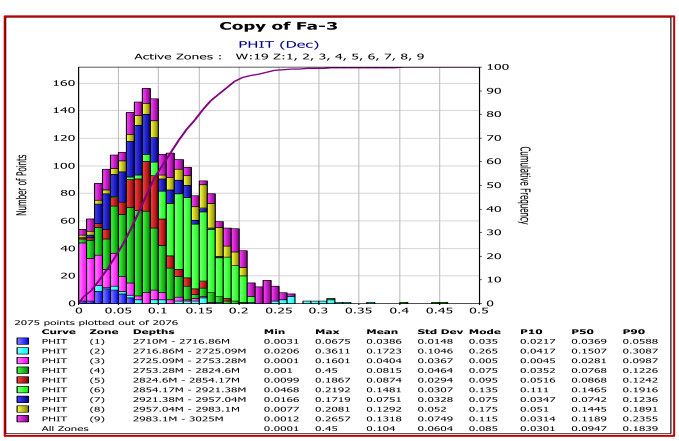

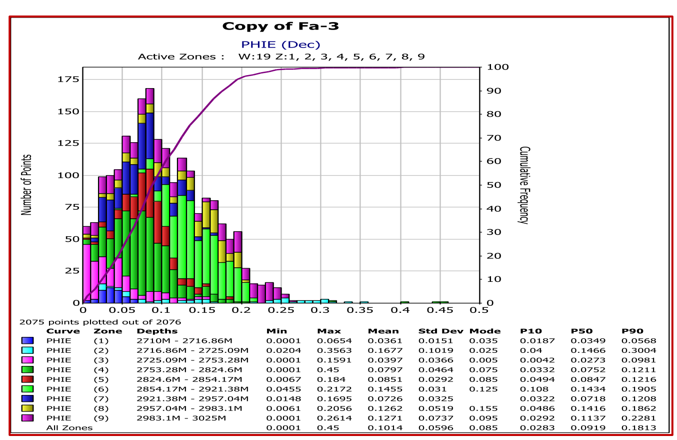

Figure 22: Total Porosity Values For Mishrif Formation In Fa-3.

Figure 23: Effective Porosity Values For Mishrif Formation In Fa-3.

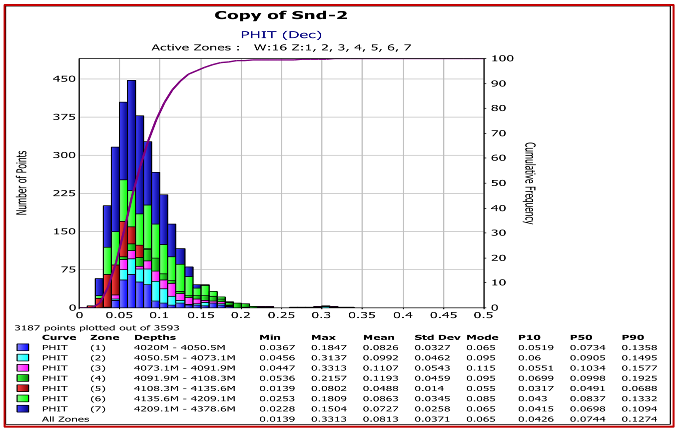

Figure 24: Total Porosity Values For Yamama Formation In Snd-2.

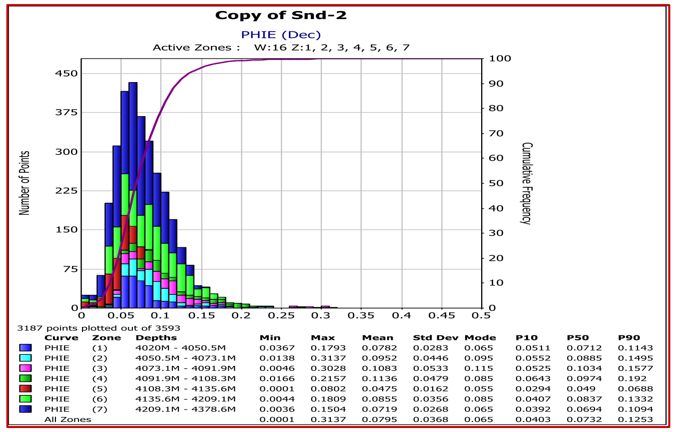

Figure 25: Effective Porosity Values For Yamama Formation In Snd-2.

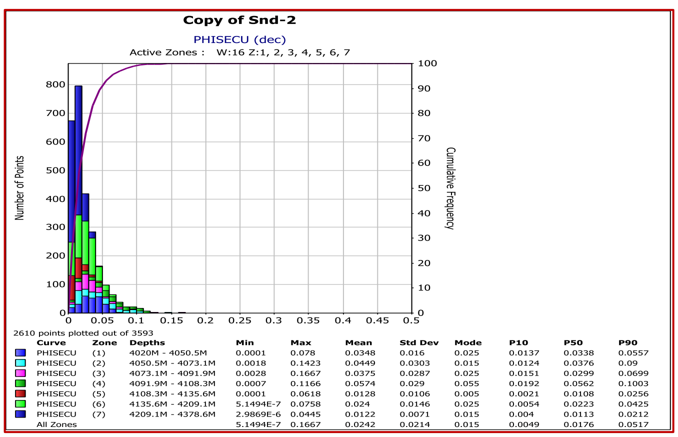

Figure 26: Secondary Porosity Values For Yamama Formation In Snd-2.

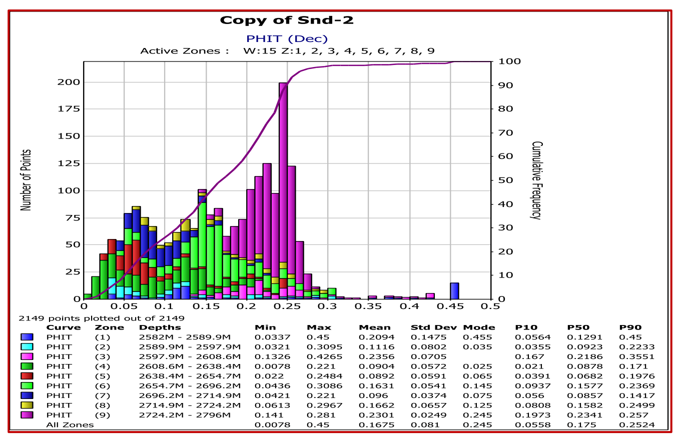

Figure 27: Total Porosity Values For Mishrif Formation In Snd-2.

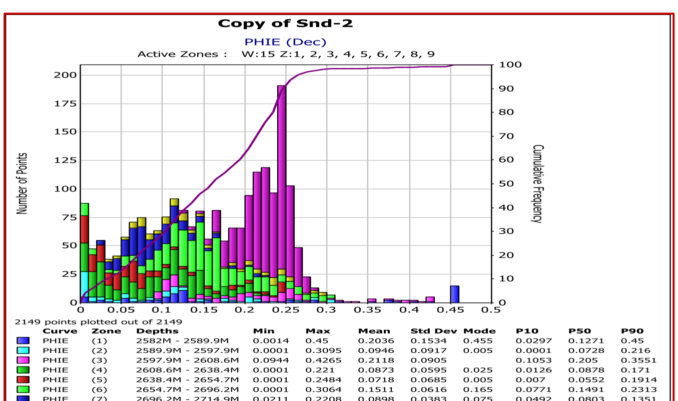

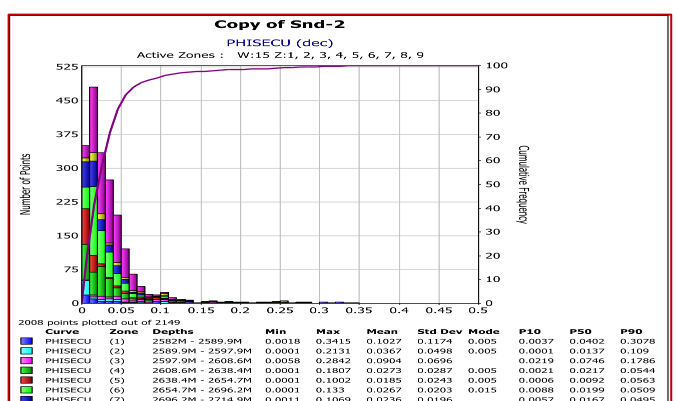

Figure 28: Effective Porosity Values For Mishrif Formation In Snd-2.

Figure 29: Secondary Porosity Values For Mishrif Formation In Snd-2.

4.4 Calculation of Water and Hydrocarbon Saturation

Water saturation for the uninvaded zone was calculated according to Archie (1942) [13]:

$$Sw = [(a * Rw) / (Rt * \_m)]^{1/n} \qquad (17)$$

Where: S_w= the water saturation (fraction); R_w= Resistivity of water formation that is previously determined from SP log (ohm-m); R_t= formation resistivity (ohm-m); a=tortuosity factor; m= cementation factor; n=saturation exponent (Archie's parameters).

Water saturation in the invaded zone (Sxo) can be simply calculated from the same equation previous mention by replacing Rw with Rmf (mud filtrate resistivity available from well log headers) and Rt with Rxo (measured resistivity of the invaded zone):

$$Sxo = [(a * Rmf) / (Rxo * \_m)]^{1/n} \qquad (18)$$

Than can be calculating the hydrocarbon saturation, by using the following equation:

$$Sh= 1 - Sw \qquad (19)$$

Movable hydrocarbon saturation was calculated based on Schlumberger (1998) [12] equation:

$$MOS= Sxo - Sw \qquad (20)$$

Whereas residual oil saturation was calculated from Schlumberger (1987) [14] as follows equation:

$$ROS= 1 - Sxo \qquad (21)$$

5. RESULTS AND DISCUSSIONS

Water and hydrocarbon saturation have been calculated using the Archie equation in (IP) software, in addition to calculations of Net pay thickness and lithology. Figures (30 to 32) show that Yamama Formation in well Fa-1 contains a high percentage and for all the zones of hydrocarbon saturation as an average of 0.5564 and the rate of residual oil saturation are 0.345, movable oil is up to 0.211. The formation has a high Net pay thickness. The lithology of formation is mainly of limestone, dolomite and shale in some depths.

Figures (33 to 35) shows the petrophysical characteristics of Mishrif Formation in well Fa-1 which contains good hydrocarbon saturation up to 0.30 and remaining hydrocarbon saturation up to 0.21 and the moveable up to 0.073. The hydrocarbon saturation is high at reservoir unit (MB) where permeability is high. The

Net pay thickness of the formation is low, in addition to the lack of moveable oil gives an evidence that the oil is heavy in the Mishrif Formation. Lithological study of formation appears that it consists mainly of interbedded limestone, dolomite and shale.

Figures (36 to 38) shows the petrophysical characteristics of Yamama Formation in well Fa-2, containing high hydrocarbon saturation of 0.5476 and residual hydrocarbon saturation of 0.478 and the moveable up to 0.0698. The Net pay thickness of the formation is high. Lithological study of formation appears that it consists mainly of interbedded limestone, dolomite and shale.

Figures (39 to 41) show that Mishrif Formation in well Fa-3, contains a good ratio for all the zones except the first and last zone of hydrocarbon saturation moveable oil up to 0.1423. The lithology of formation is mainly limestone as well as dolomite and shale.

Figures (42 to 44) show that Yamama Formation in well Snd-2, contains a high proportion of all the zones of hydrocarbon saturation except the seventh and part of the sixth zone as an average up to 0.4112 and the rate of remaining oil saturation up to 0.4377, and the moveable oil is none. The formation has a middle of Net pay thickness. The lithology of formation is mainly of limestone, dolomite and shale in some depths.

Figures (45 to 47) shows the petrophysical characteristics of Mishrif Formation in well Snd-2, containing only hydrocarbon saturation in the upper reservoir unit (MA) up to 0.357 and residual hydrocarbon saturation 0.291 and the moveable up to 0.0667. Hydrocarbon saturation is inconsiderable at the remaining zones. The Net pay thickness of the formation is inconsiderable. The lithology of formation is mainly limestone, dolomite and shale.

From comparing of Yamama Formation in the Faiha and Sindibad fields, that Yamama Formation in the Faiha field is better than Yamama Formation in the Sindibad field according to petrophysical properties and hydrocarbon saturation, as well as when comparing Mishrif Formation of the Faiha and Sindibad fields shows that Mishrif Formation in the Sindibad field is better than Mishrif Formation in the Faiha field according to petrophysical properties and hydrocarbon saturation. In comparison, between Mishrif and Yamama formations, it shows that petrophysical characteristics of Yamama Formation are better than Mishrif Formation, as shown in Figures (48 and 49).

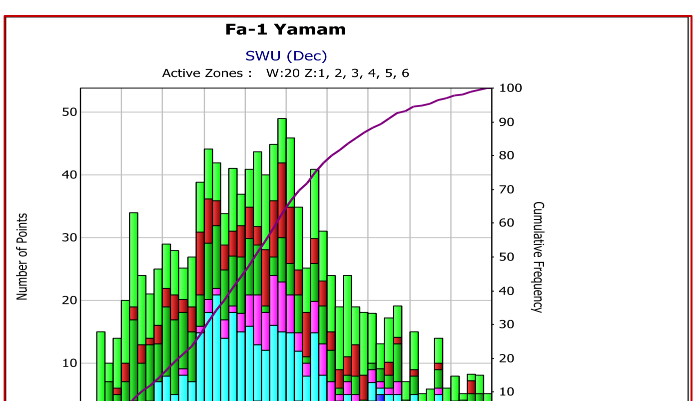

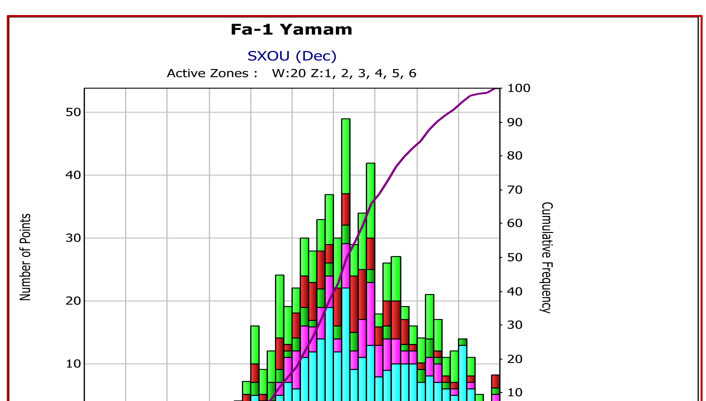

Figure 30: Statistical Analysis Of Water Saturation Values For Yamama Formation In Fa-1.

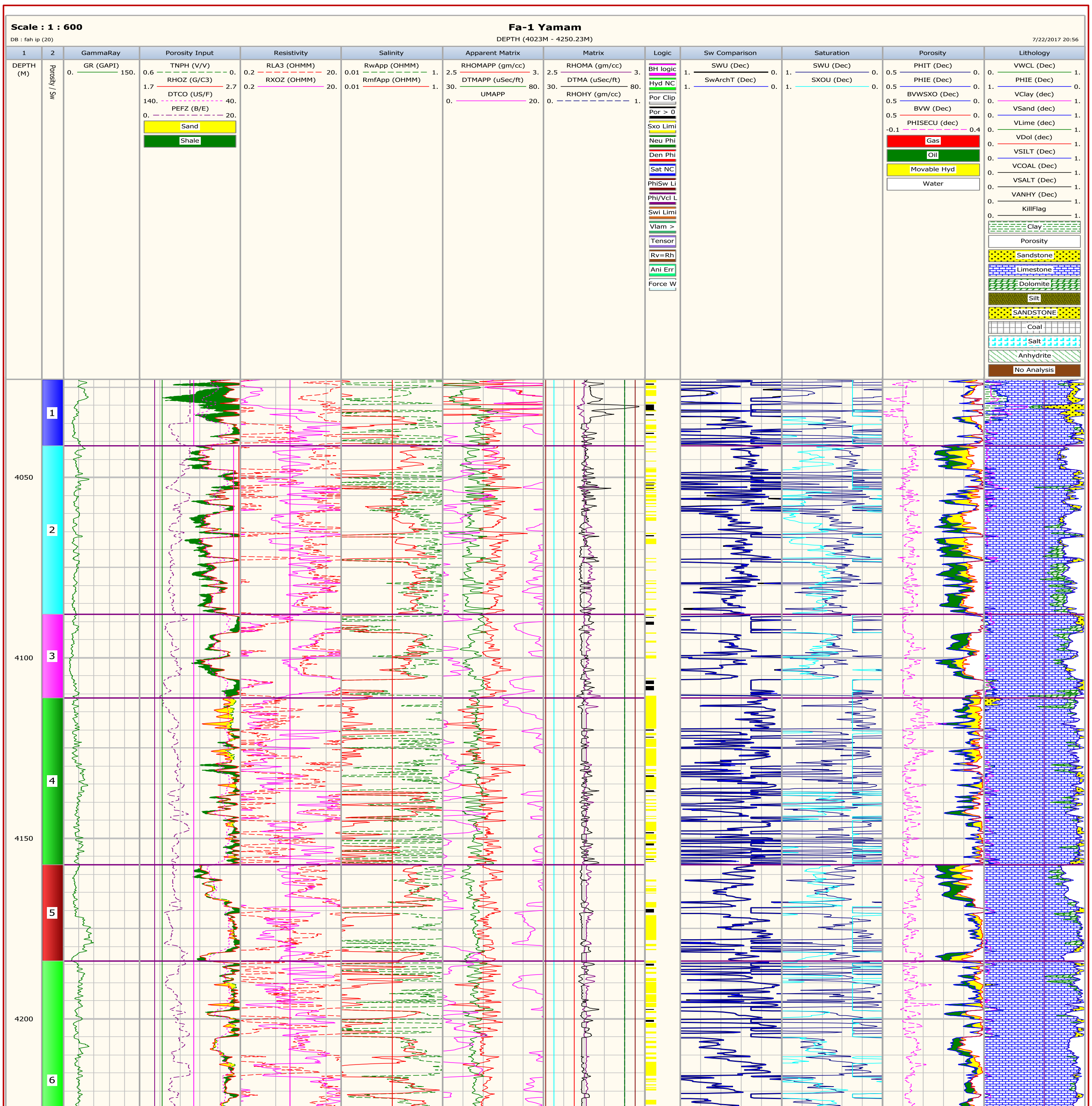

Figure 31: Water Saturation And Porosity For Yamama Formation In Fa-1.

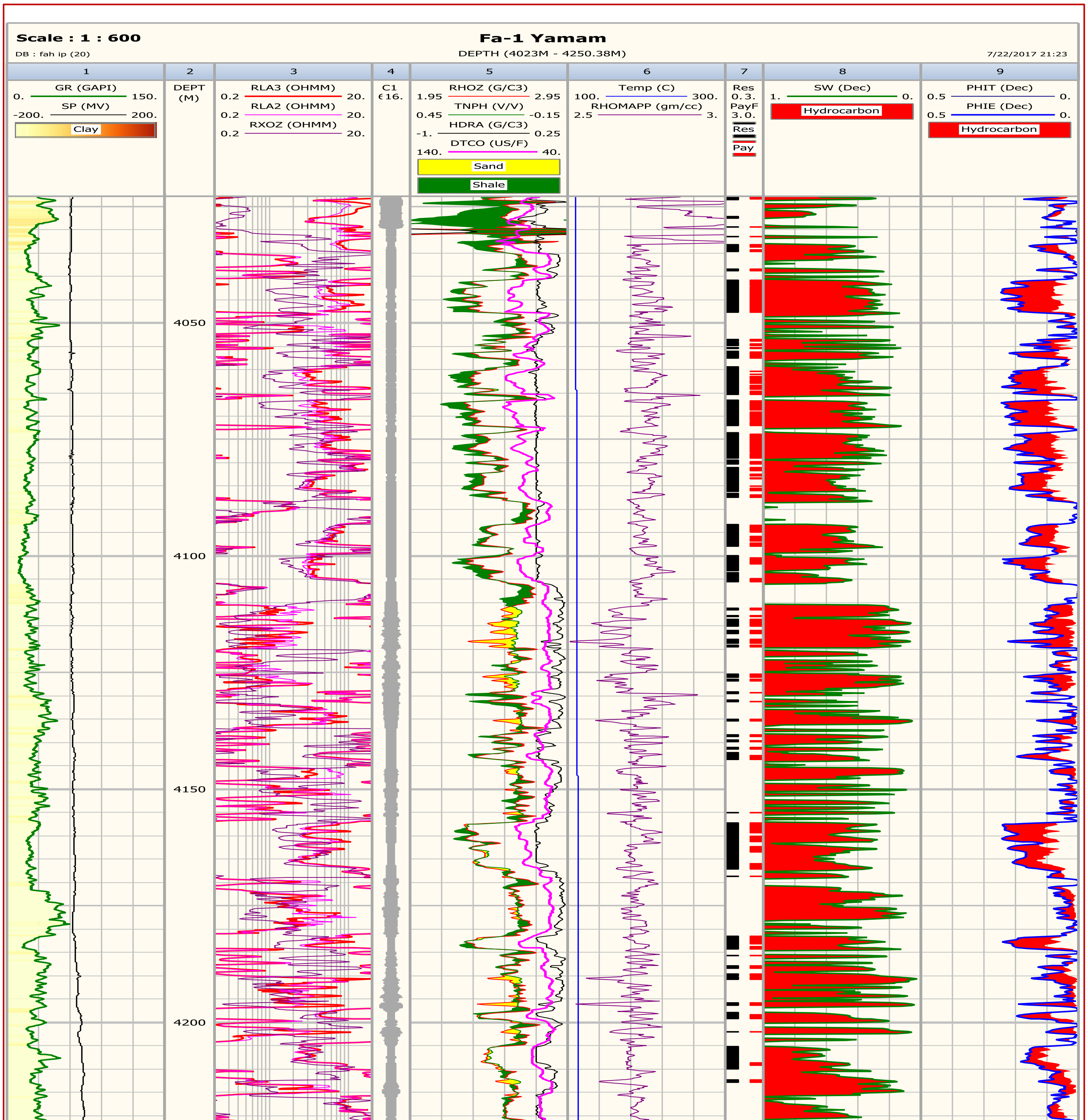

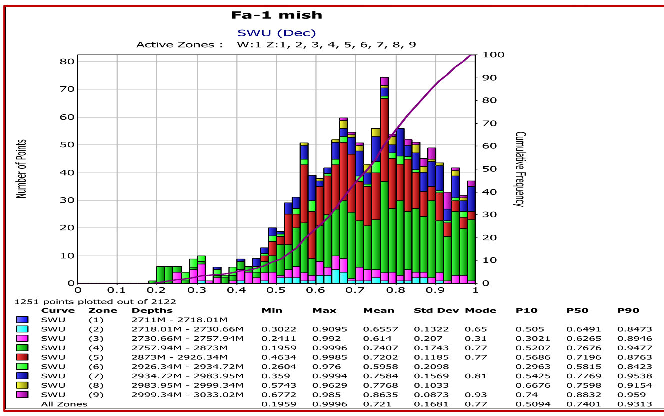

Curve	Zone	Depths	Min	Max	Mean	Std Dev	Mode	P10	P50	P90
SWU	(1)	2711M - 2718.01M								
SWU	(2)	2718.01M - 2730.66M	0.3022	0.9095	0.6557	0.1322	0.65	0.505	0.6491	0.8473
SWU	(3)	2730.66M - 2757.94M	0.2411	0.992	0.614	0.207	0.31	0.3021	0.6265	0.8946
SWU	(4)	2757.94M - 2873M	0.1959	0.9996	0.7407	0.1743	0.77	0.5207	0.7676	0.9477
SWU	(5)	2873M - 2926.34M	0.4634	0.9985	0.7202	0.1185	0.77	0.5686	0.7196	0.8763
SWU	(6)	2926.34M - 2934.72M	0.2604	0.976	0.5958	0.2098		0.2963	0.5815	0.8423
SWU	(7)	2934.72M - 2983.95M	0.359	0.9994	0.7584	0.1569	0.81	0.5425	0.7769	0.9538
SWU	(8)	2983.95M - 2999.34M	0.5743	0.9629	0.7768	0.1033		0.6676	0.7598	0.9154
SWU	(9)	2999.34M - 3033.02M	0.6772	0.985	0.8635	0.0873	0.93	0.74	0.8832	0.959
All Zones			0.1959	0.9996	0.721	0.1681	0.77	0.5094	0.7401	0.9313

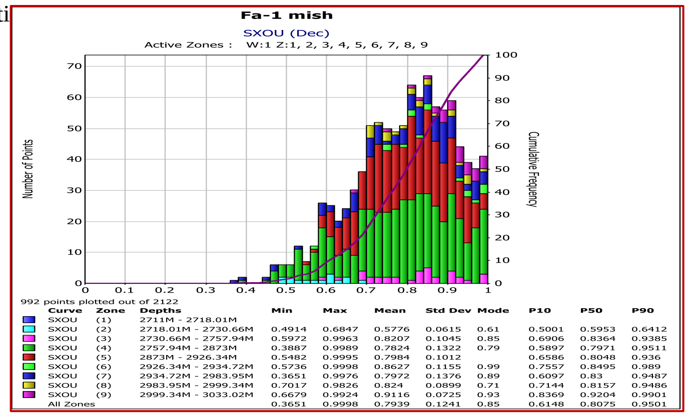

Curve	Zone	Depths	Min	Max	Mean	Std Dev	Mode	P10	P50	P90
SXOU	(1)	2711M - 2718.01M								
SXOU	(2)	2718.01M - 2730.66M	0.4914	0.6847	0.5776	0.0615	0.61	0.5001	0.5953	0.6412
SXOU	(3)	2730.66M - 2757.94M	0.5972	0.9963	0.8207	0.1045	0.85	0.6906	0.8364	0.9385
SXOU	(4)	2757.94M - 2873M	0.3887	0.9989	0.7824	0.1322	0.79	0.5897	0.7971	0.9511
SXOU	(5)	2873M - 2926.34M	0.5482	0.9995	0.7984	0.1012		0.6586	0.8048	0.936
SXOU	(6)	2926.34M - 2934.72M	0.5736	0.9998	0.8627	0.1155	0.99	0.7557	0.8495	0.989
SXOU	(7)	2934.72M - 2983.95M	0.3651	0.9976	0.7972	0.1376	0.89	0.6097	0.83	0.9487
SXOU	(8)	2983.95M - 2999.34M	0.7017	0.9826	0.824	0.0899	0.71	0.7144	0.8157	0.9486
SXOU	(9)	2999.34M - 3033.02M	0.6679	0.9924	0.9116	0.0725	0.93	0.8369	0.9204	0.9901
All Zones			0.3651	0.9998	0.7939	0.1241	0.85	0.6148	0.8075	0.9501

Figure 33: Statistical Analysis Of Water Saturation Values For Mishrif Formation In Fa-1.

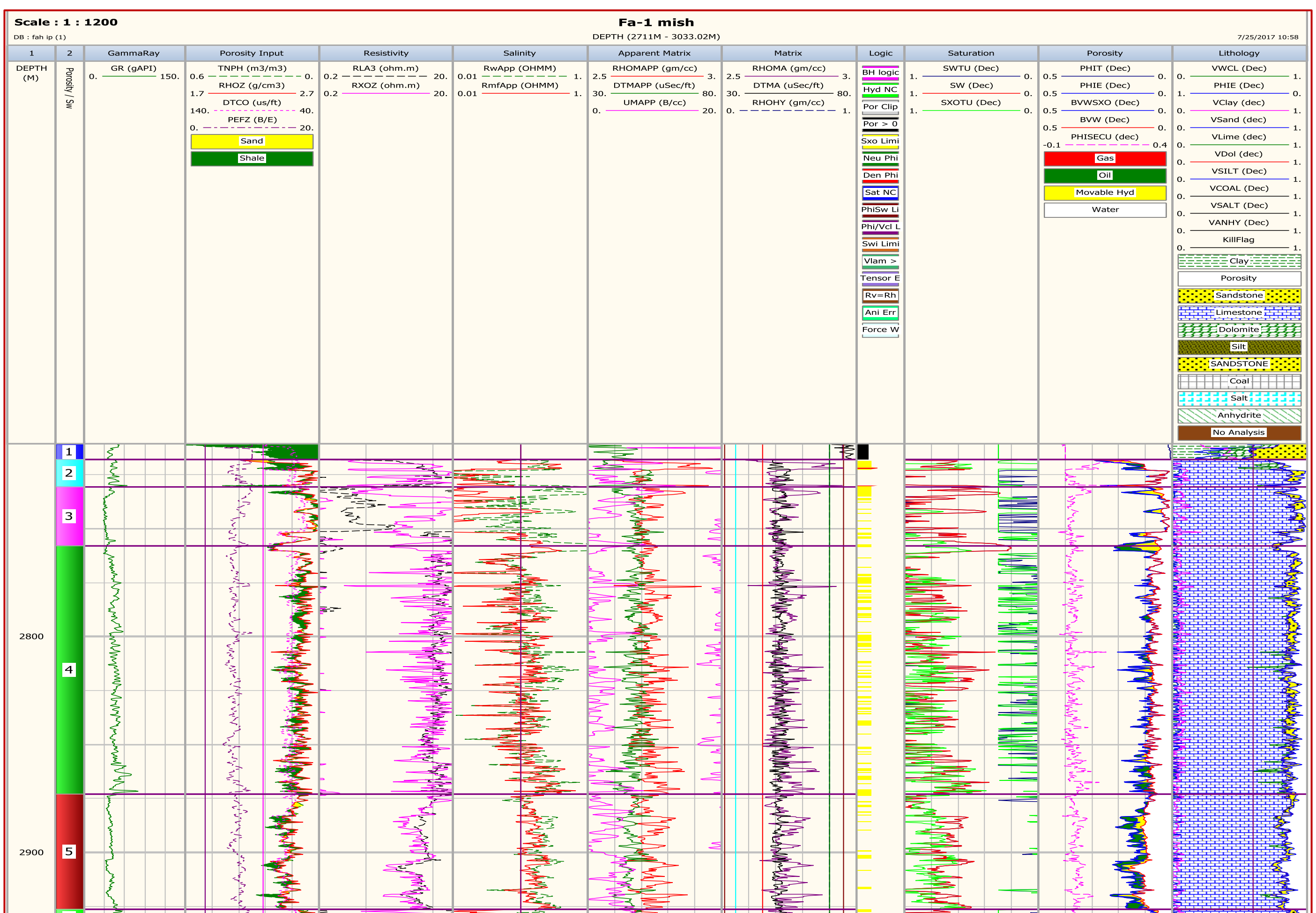

Figure 34: Water Saturation And Porosity For Mishrif Formation In Fa-1.

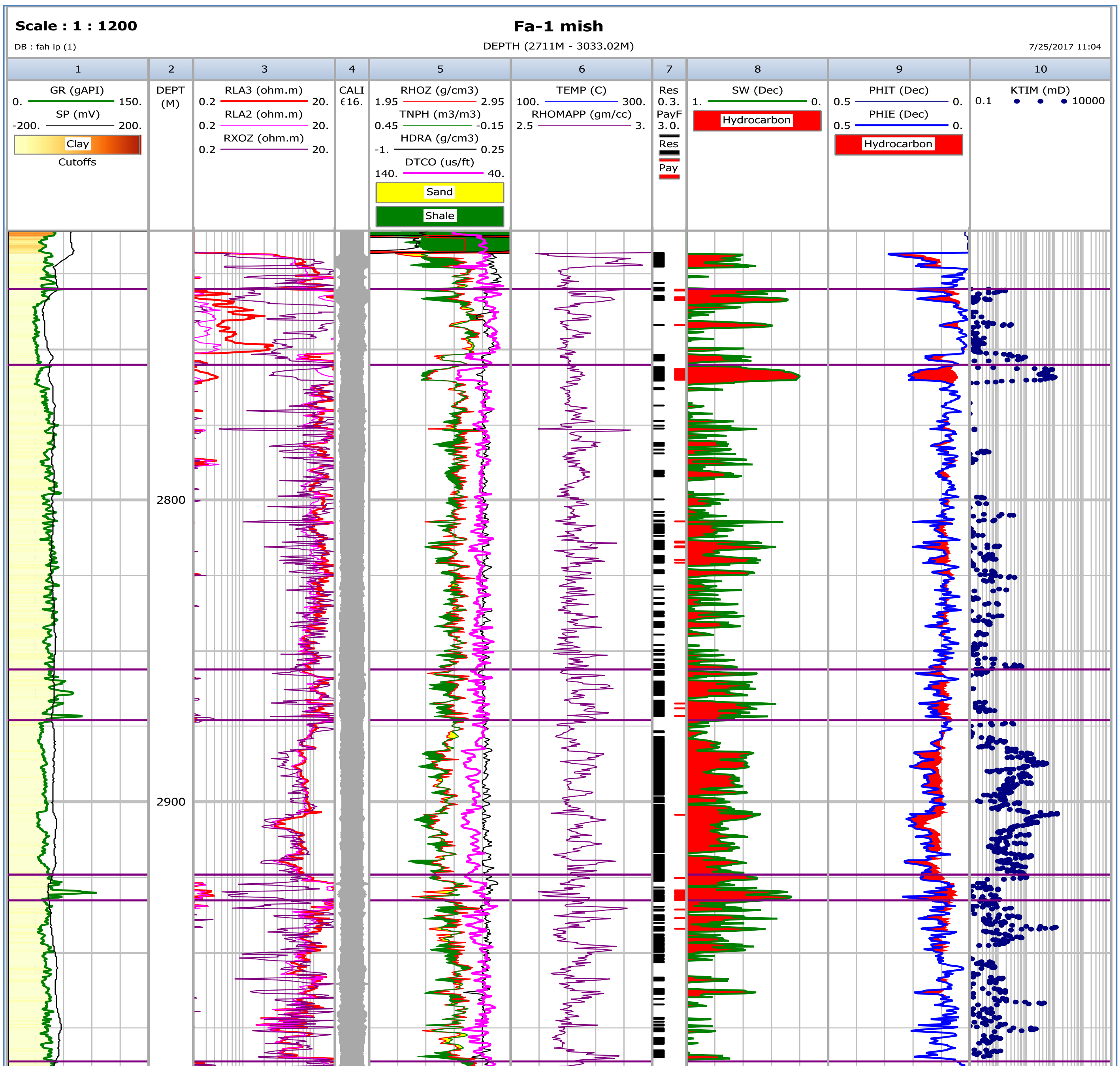

Figure 35: Computer Processed Interpretation (CPI) for Mishrif Formation In Fa-1.

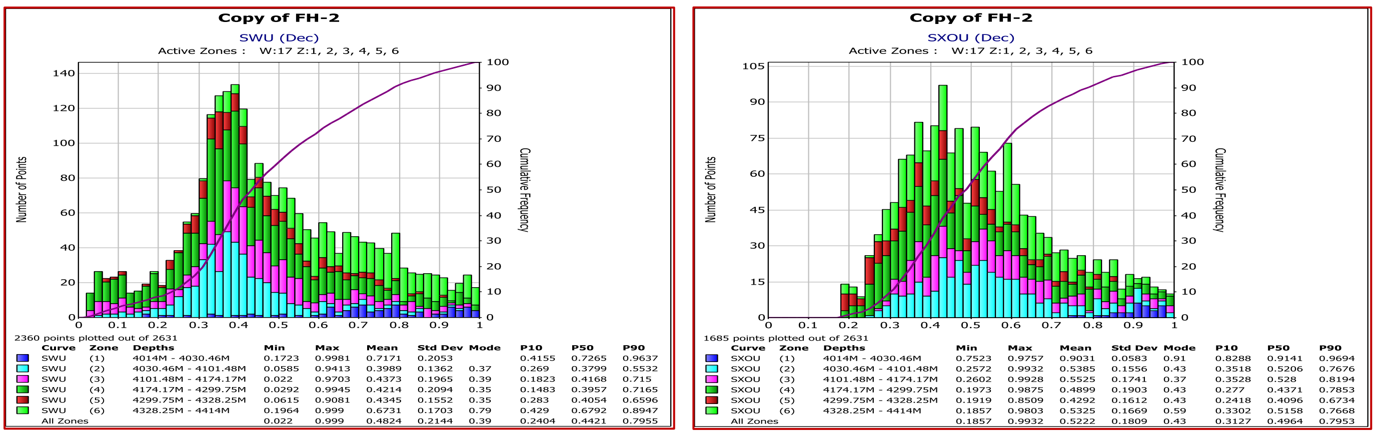

Figure 36: Statistical Analysis Of Water Saturation Values For Yamama Formation In Fa-2.

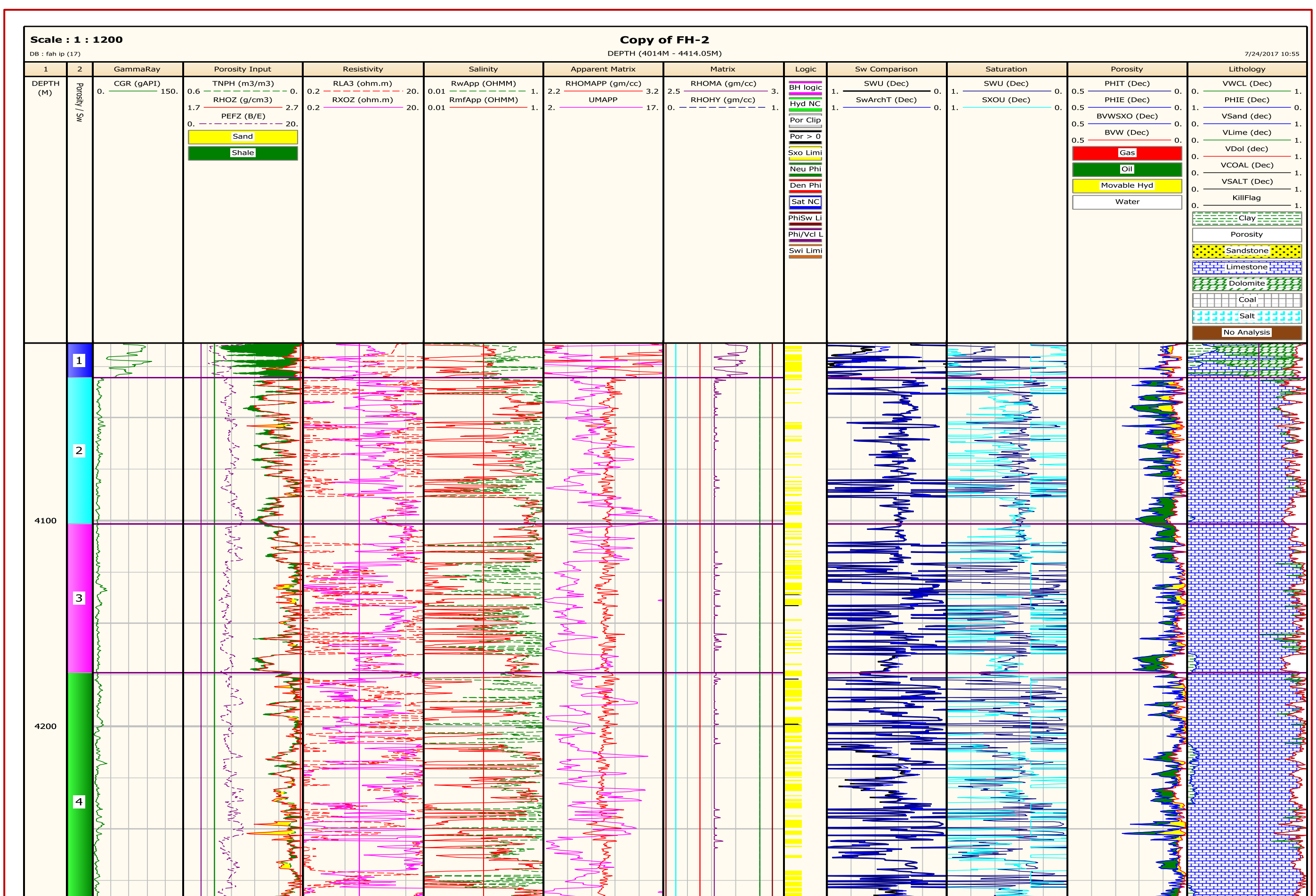

Figure 37: Water Saturation And Porosity For Yamama Formation In Fa-2.

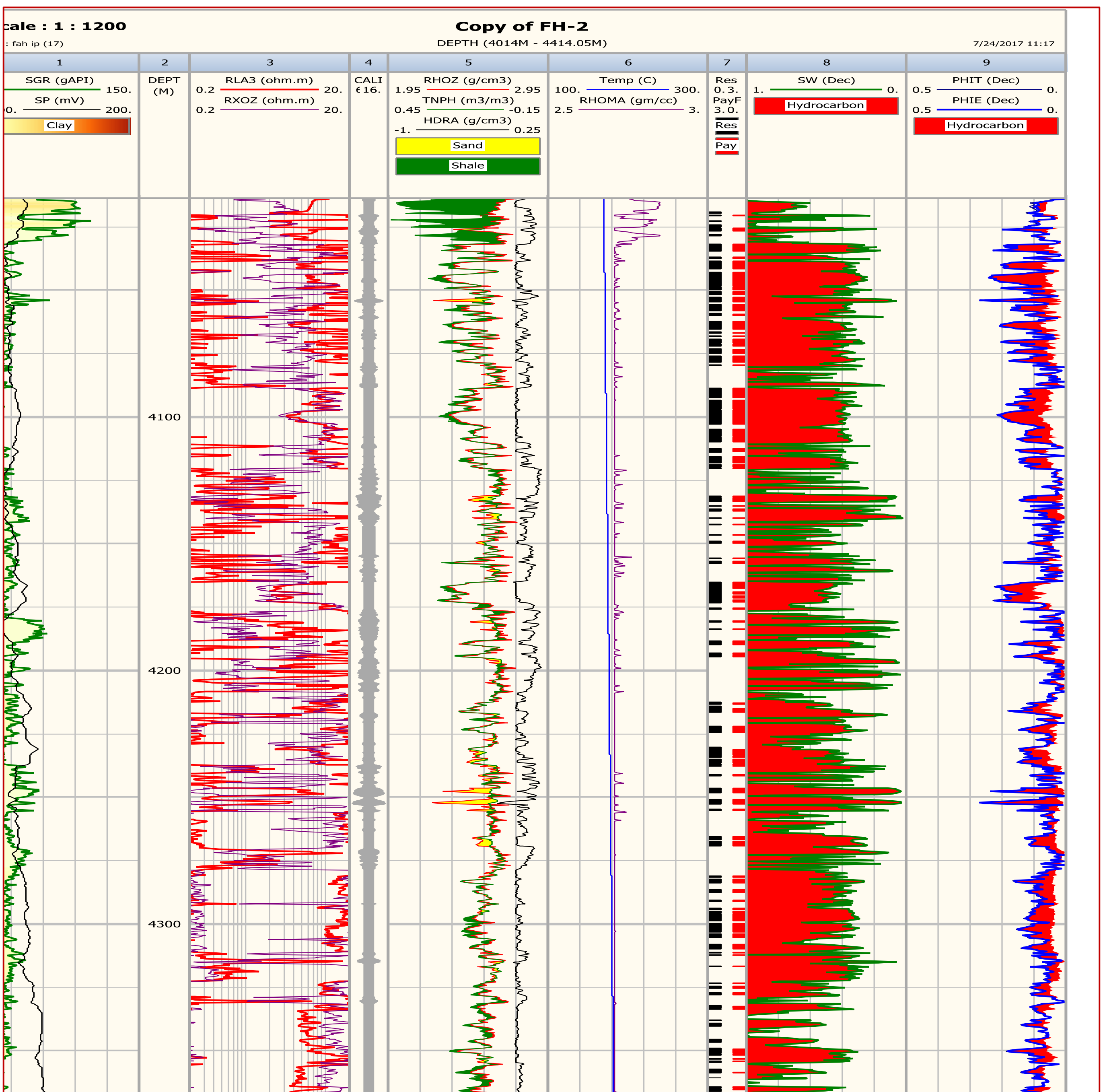

Figure 38: Computer Processed Interpretation (CPI) For Yamama Formation In Fa-2.

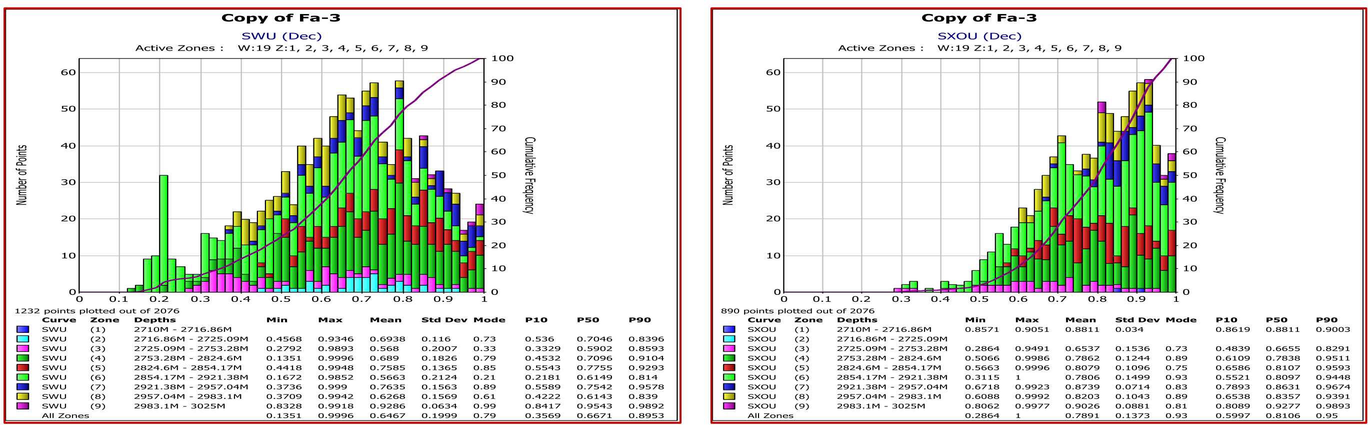

Figure 39: Statistical Analysis Of Water Saturation Values For Mishrif Formation In Fa-3.

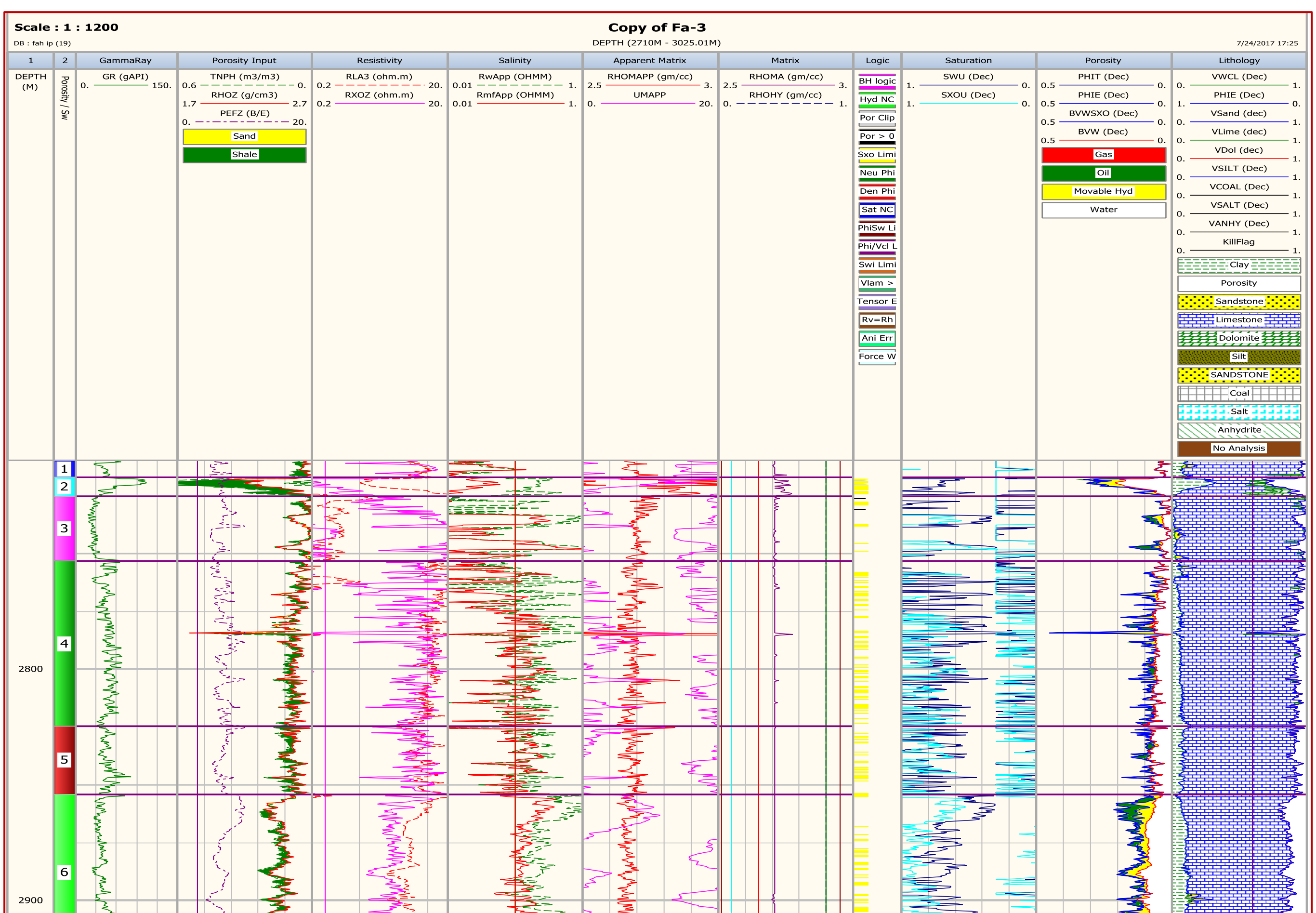

Figure 40: Water Saturation And Porosity For Mishrif Formation In Fa-3.

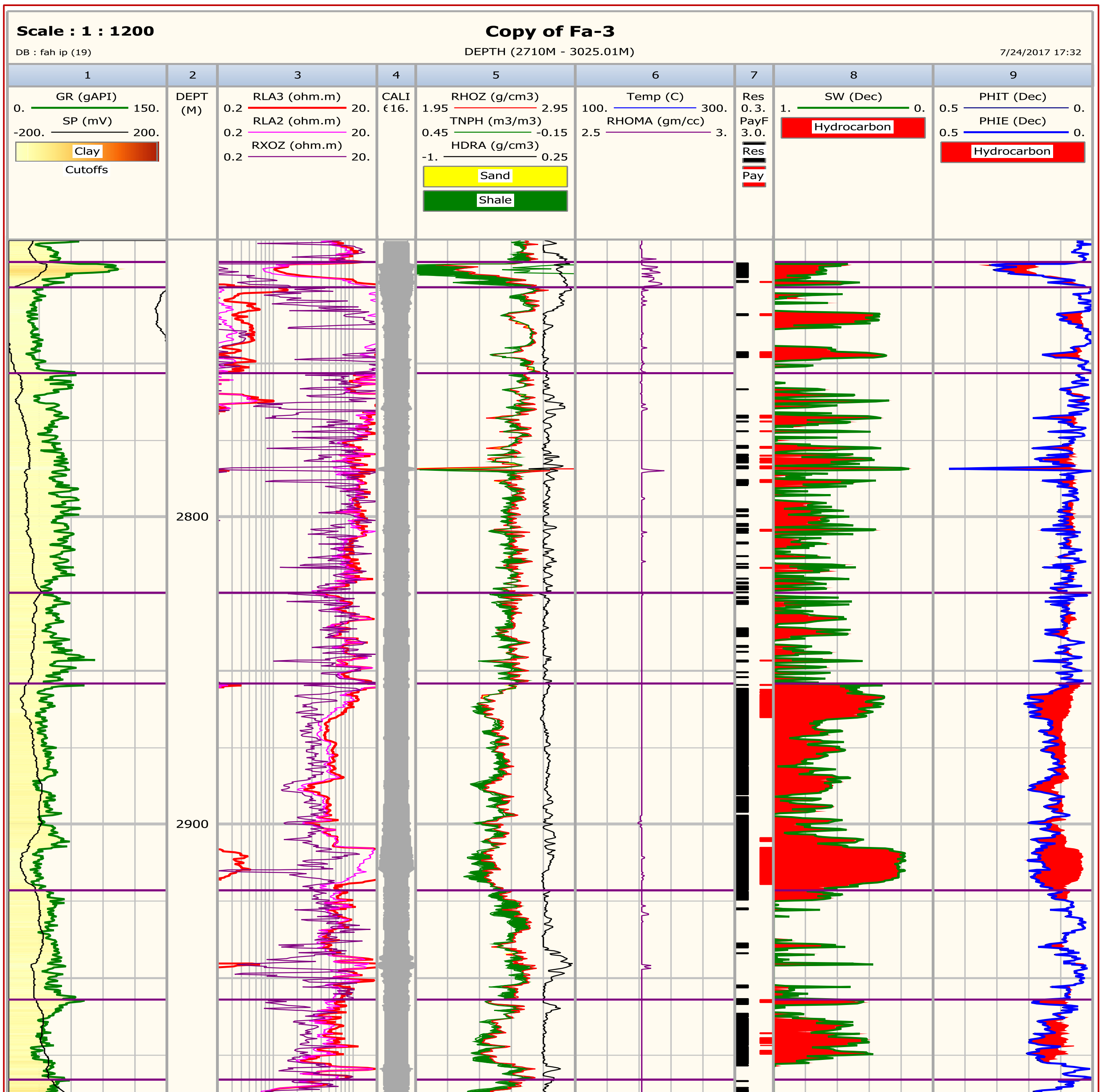

Figure 41: Computer Processed Interpretation (CPI) for Mishrif Formation In Fa-3.

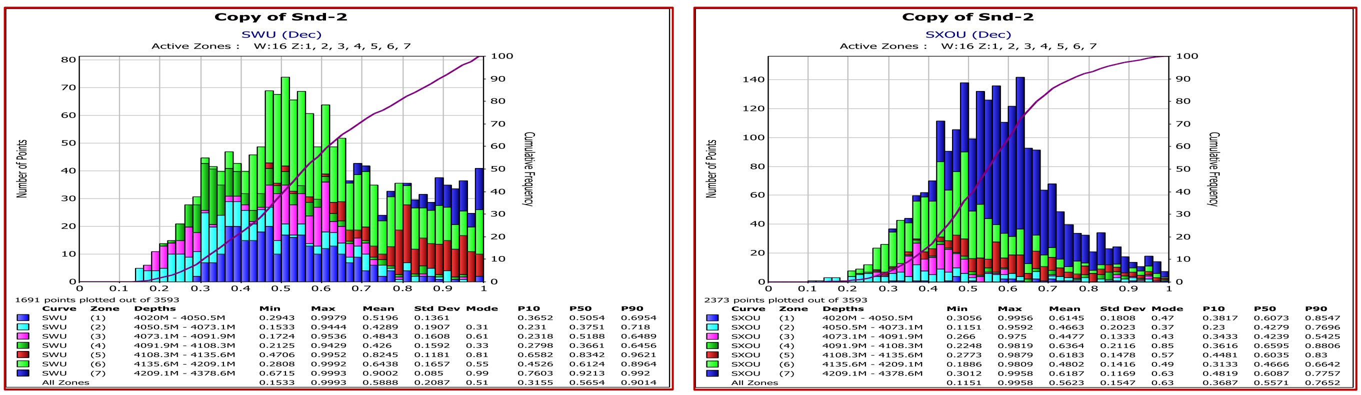

Figure 42: Statistical Analysis Of Water Saturation Values For Yamama Formation In Snd-2.

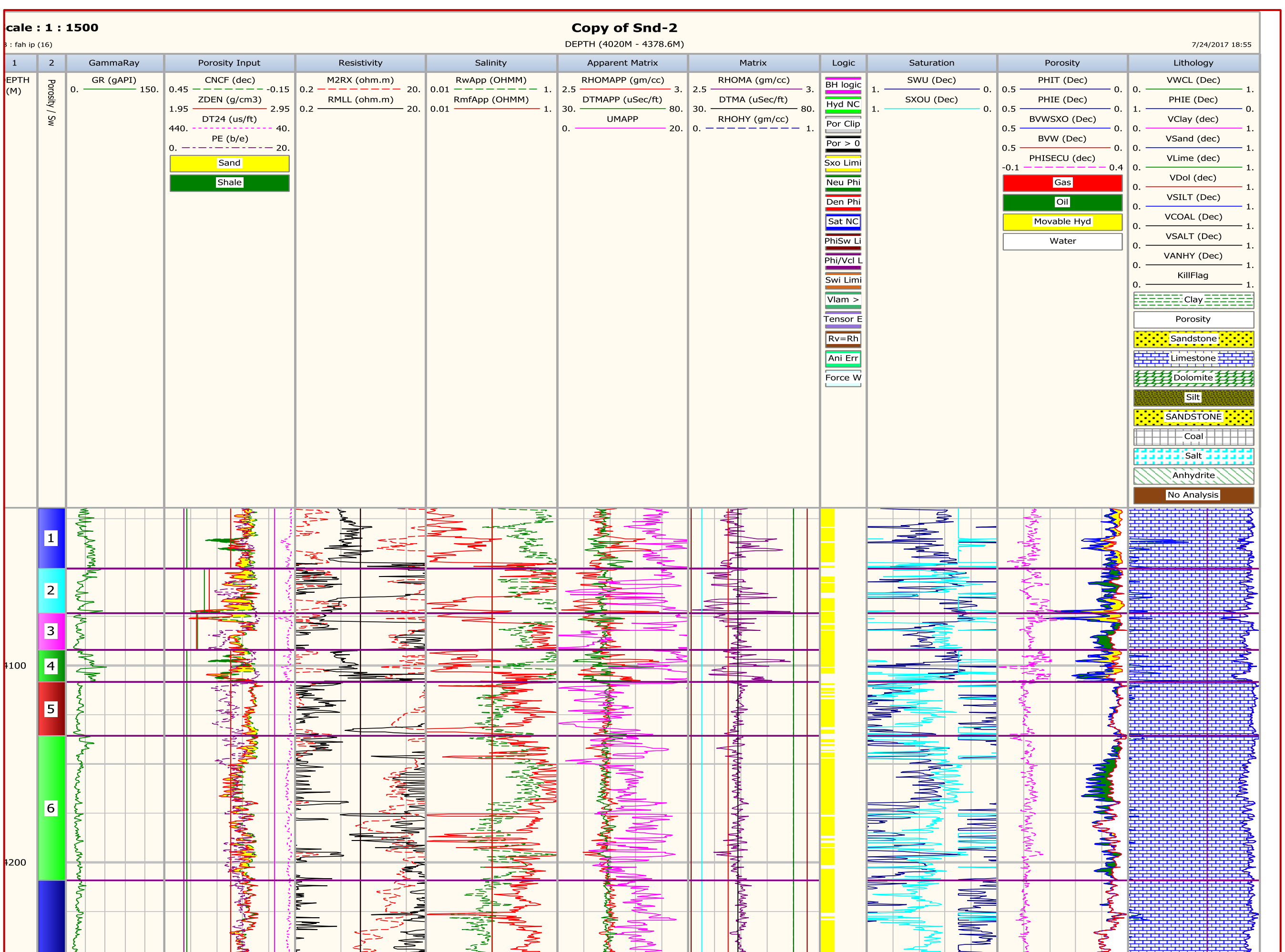

Figure 43: Water Saturation And Porosity For Yamama Formation In Snd-2.

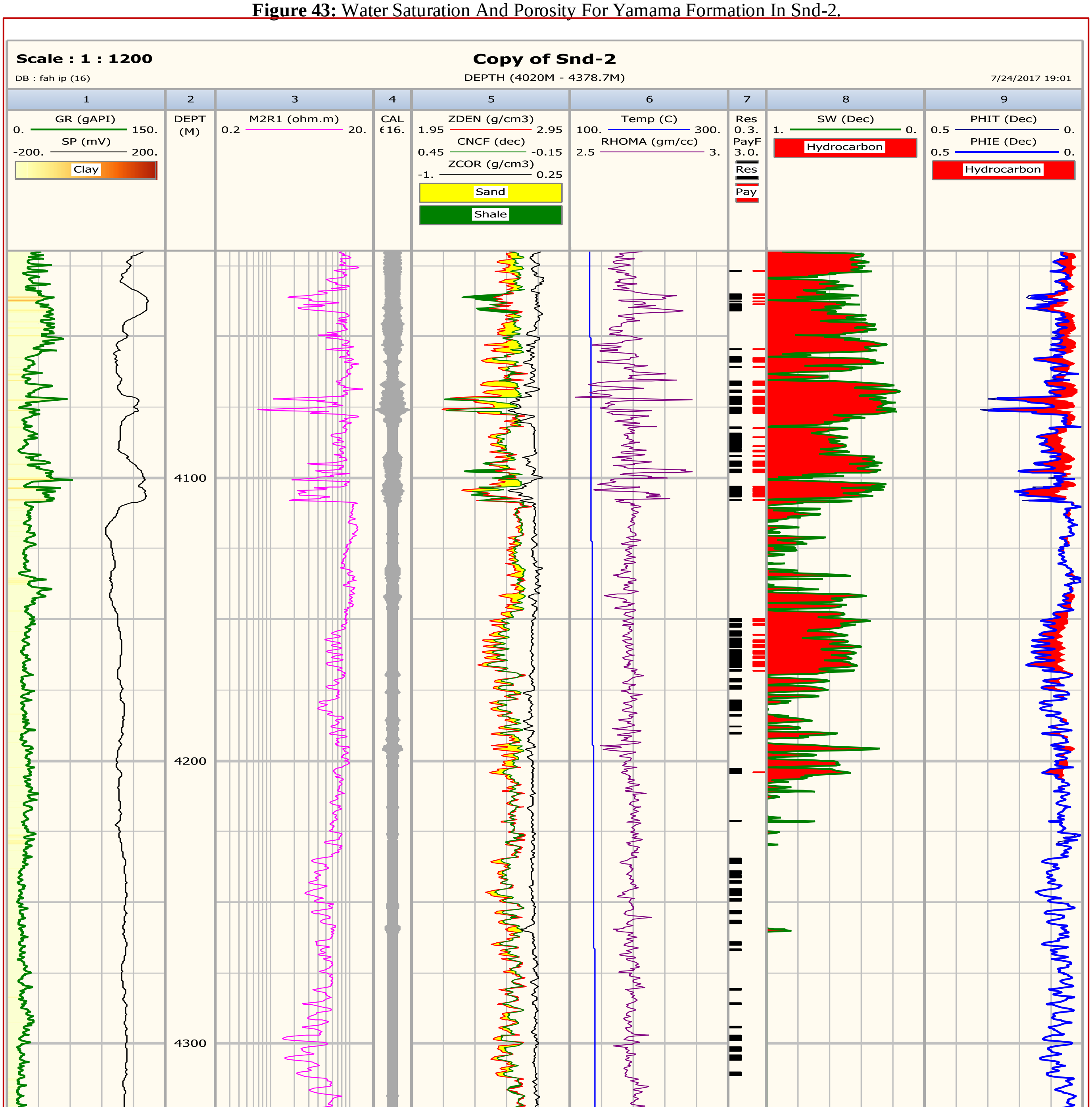

Figure 44: Computer Processed Interpretation (CPI) For Yamama Formation In Snd-2.

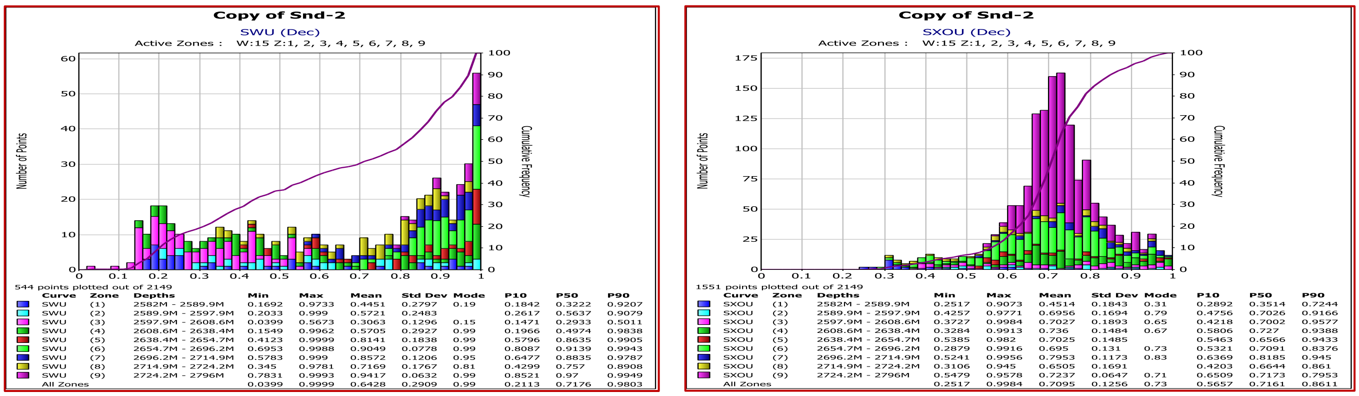

Figure 45: Statistical Analysis Of Water Saturation Values For Mishrif Formation In Snd-2.

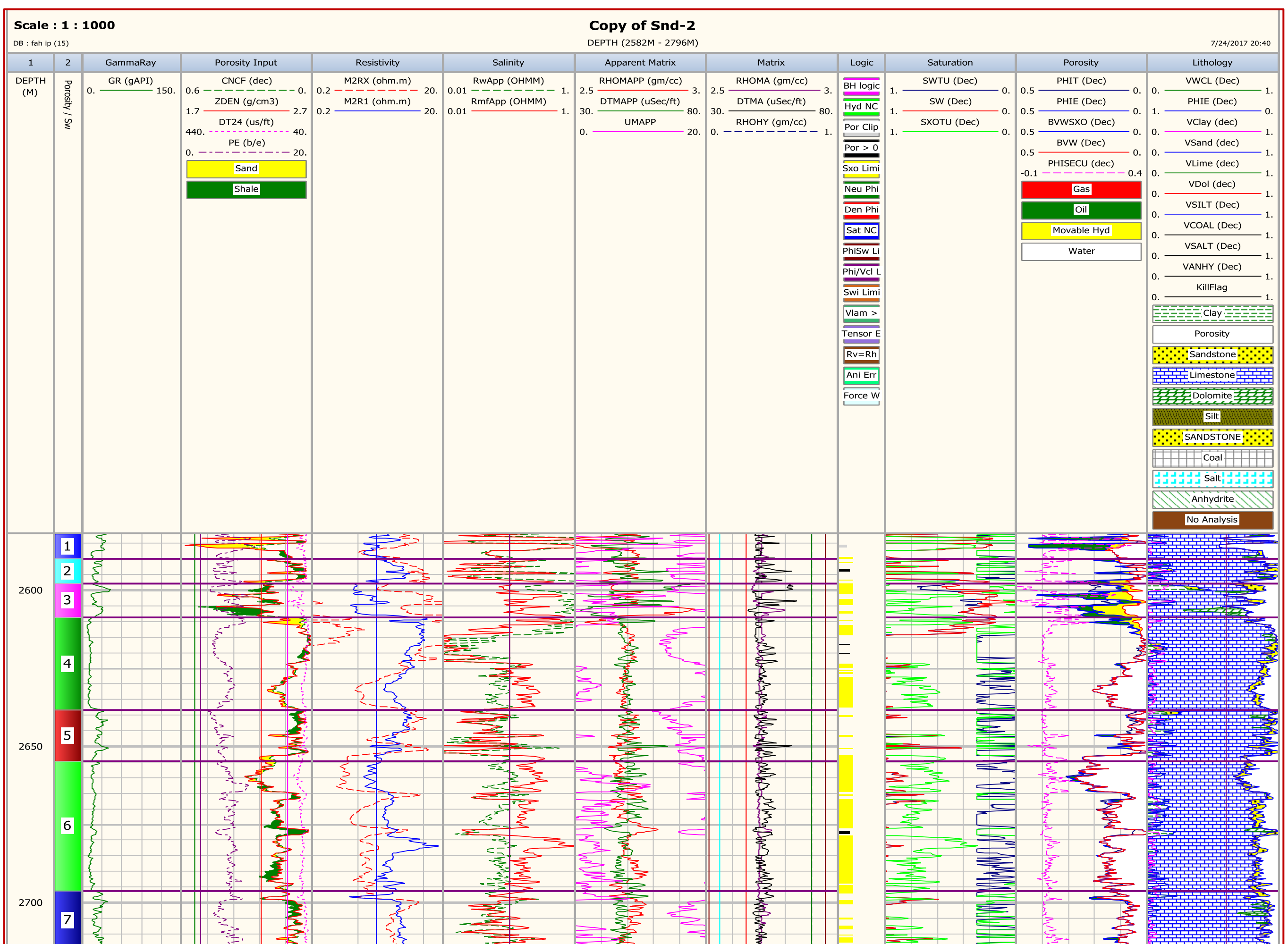

Figure 46: Water Saturation And Porosity For Mishrif Formation In Snd-2

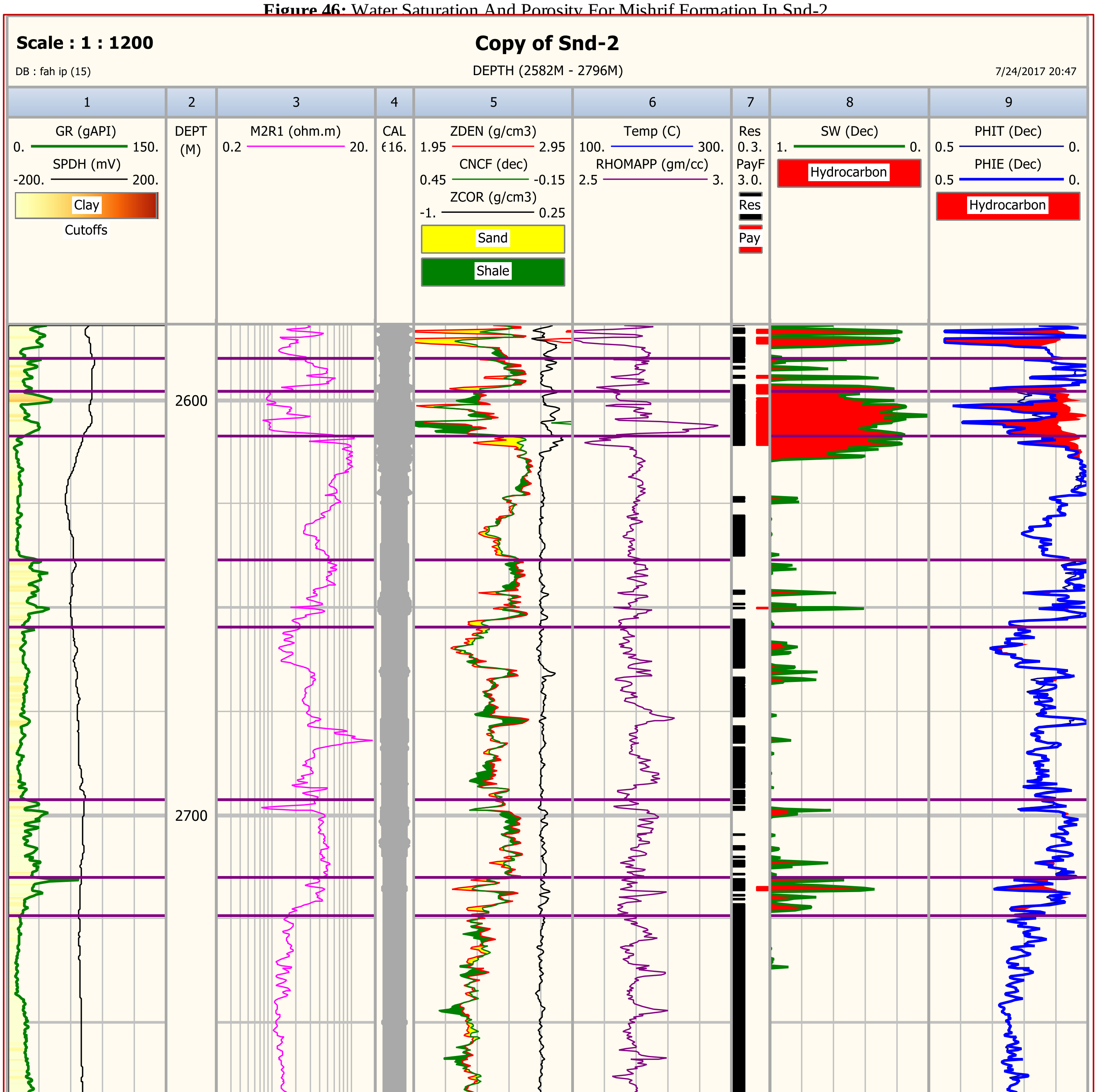

Figure 47: Computer Processed Interpretation (CPI) for Mishrif Formation In Snd-2.

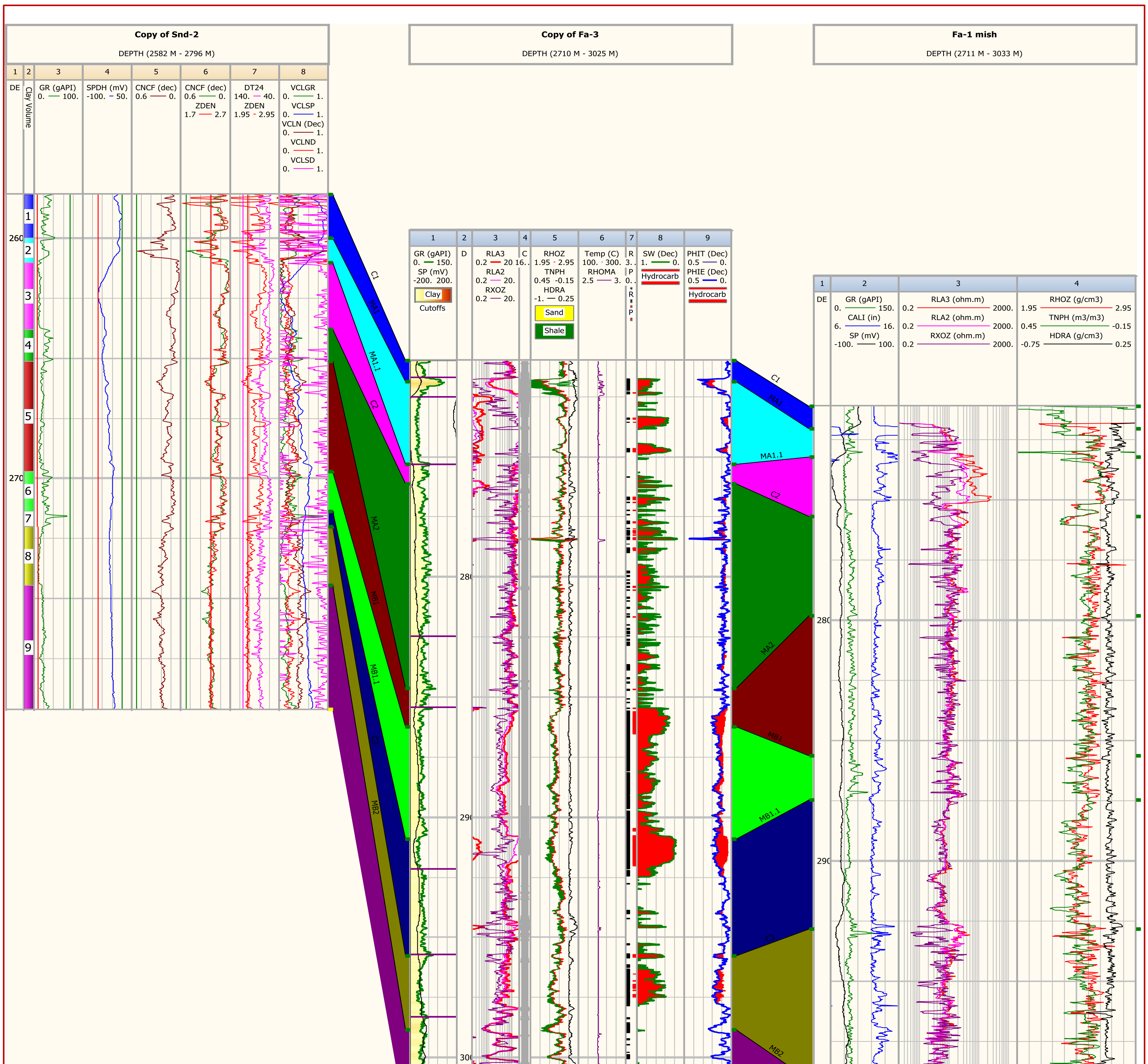

Figure 48: Correlation Of Mishrif Formation Between The Wells Of The Study Area.

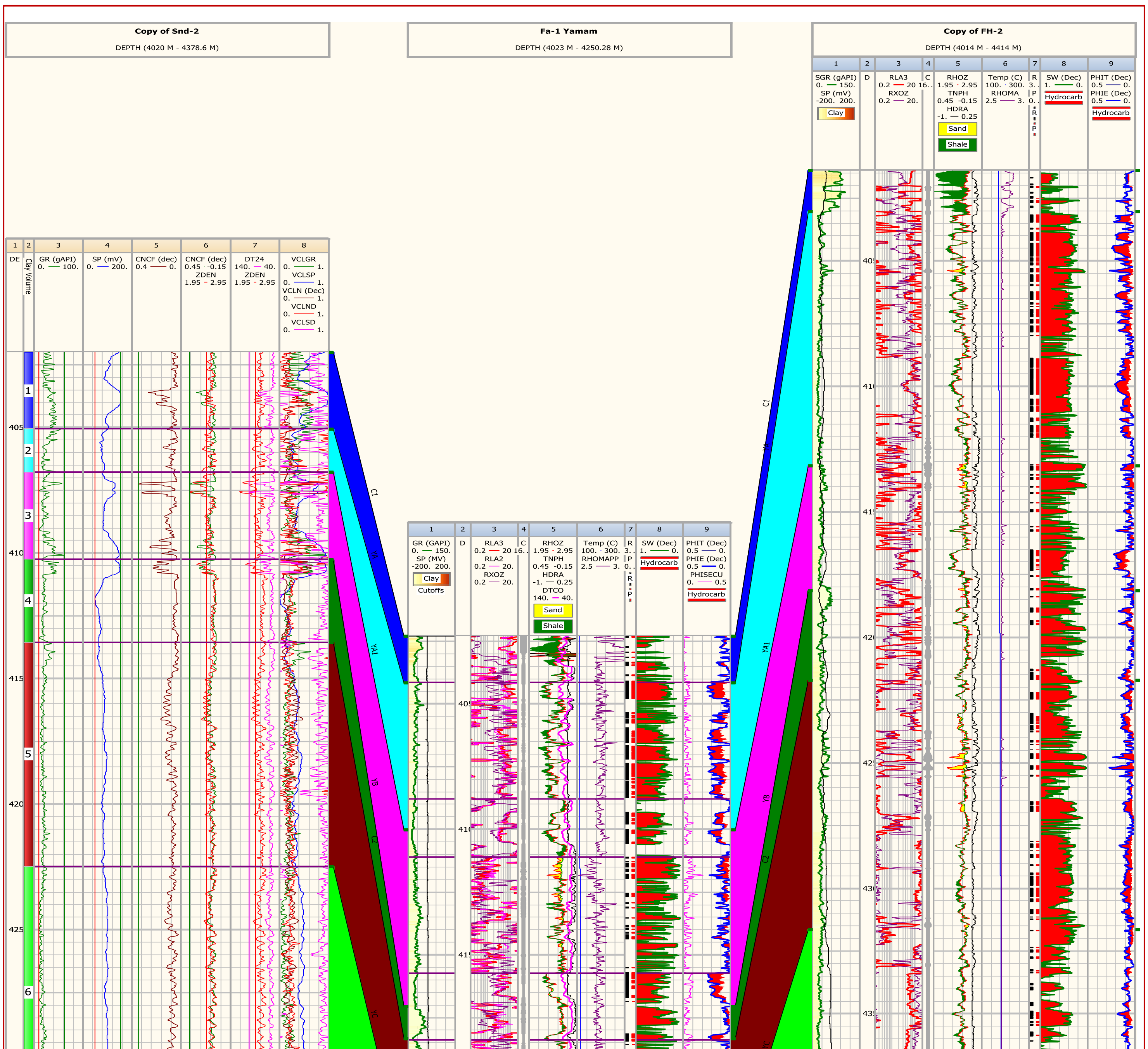

Figure 49: Correlation Of Yamama Formation Between The Wells Of The Study Area.

6. CONCLUSIONS

According to this study and depending on the petrophysical properties the shale volume has been calculated by using (IP) software the results of calculating the volume of shale show an increase in volume more than (10%) in most depth intervals. Statistical analysis shows that the least percentage of shale was in Yamama Formation in well Fa-2 and the highest percentage was in Yamama Formation in Fa-1. Layers boundaries have been determined and divide the formations into many zones based on behavior of well logs and shale volume. Mishrif Formation in Faiha Field is divided into nine zones and nine zones in Sindibad Field, while Yamama Formation is divided into six zones in Faiha Field and seven zones in Sindibad Field.

According to Computer processed interpretation (CPI), Mishrif Formation are characterized by primary porosity (effective) in well Snd-2 better than Fa-1 and Fa-3 and secondary porosity little or none, while Yamama Formation is characterized by primary porosity (effective) values in well Fa-1 better than Fa-2 and Snd-2 and total porosity of the Yamama Formation is high, while secondary porosity little or none in some depths.

In general, Mishrif Formation in well Snd-2 is characterized by good hydrocarbon saturation (0.30) and the residual and movable saturation are 0.21 and 0.073, respectively. Results also referred that hydrocarbon saturation and permeability in some ranges of the formation especially in MB unit is very high, in addition to the low movable oil and this may indication of the heavy oil in the formation. In general, the reservoir characteristics of Yamama Formation in Fa-1 better than Fa-2 and Snd-2. Lithological study of Mishrif Formation appears that it consists mainly of interbedded limestone, dolomite and shale. While interpretations of well logs of Yamama Formation in well Fa-1 indicated high hydrocarbon saturation (an average of 0.556). The residual oil saturation and movable oil are 0.345 and 0.211, respectively. In general, the reservoir characteristics of Yamama Formation in Fa-1 are better than Fa-2 and Snd-2. Lithological study of Yamama Formation consists mainly of interbedded limestone, dolomite and shale in some depths.

REFERENCES

[1] O. Catuneanu, Principles of Sequence Stratigraphy. Department of Earth and Atmospheric Sciences, University of Alberta, Canada. First Edition Elsevier Science Publishers Company INC., 375 (2006).

[2] M. Gonfalini, The Fundamental Role of Formation evaluation in the E&P Process. STYPED "Sponsor Team for young petroleum Engineers Development"; 28 (2005).

[3] D.W. Hilchie, Applied open hole log interpretation. Colorado, Inc., 309 (1978).

[4] Z. Basseoni (1994) Theory, Measurement and Interpretation of well logs Society of Petroleum Engineers, **4**, Richardson, USA, 372.

[5] Schlumberger, Well Evaluation Conference, Libya, Service Techniques Schlumberger, France, 2-6 (1970).

[6] Schlumberger, The Essential of log Interpretation Practice, Services Technique Schlumberger, France, 54 (1972).

[7] Schlumberger (1974) Log Interpretation, **II**, Applications, New York.

[8] Dresser Atlas, Log Interpretation Charts. Houston. Dresser Industries, Inc., 107 (1979).

[9] Schlumberger, Log interpretation charts, USA (1984).

[10] D. Tiab. And E. C. Donaldson, Petrophysics theory and practice of measuring reservoir rock and fluid transport properties; Houston, Texas, 706. (1996).

[11] M. R. J. Wyllie, A. R. Gregory and G. H. Gardner (1958) An experimental investigation of the factors affecting elastic wave velocities in porous media; Geophysics, **23**, 495-493.

[12] Schlumberger, Cased Hole Log Interpretation Principles / Applications, Houston, Schlumberger Wireline and Testing, 198 (1998).

[13] G. E. Archie (1942) The Electrical Resistivity Log as an Aid in determining some Reservoir Characteristics; AIME, **146**, 54.

[14] Schlumberger, Log interpretation charts, USA (1987).

دراسة الخواص البتروفيزيائية لتكويني المشرف واليمامة في حقول مختارة، جنوب العراق

[1]آمنة مال الله حنظل، [2]حسين عليوي جفيت، [3]نوفل عدنان دحام [4]ورغد بشير

[1و4] قسم علوم الأرض، كلية العلوم، جامعة البصرة، البصرة، العراق

[2و3] قسم هندسة النفط والغاز، كلية هندسة النفط والغاز، جامعة البصرة للنفط والغاز، البصرة، العراق

Email: [1]amhgeo@gmail.com, [2]hussein.aliwi@buog.edu.iq, [3]Nawfal.adnan@buog.edu.iq

الخلاصة:

الخصائص المكمنية تتطلب معرفة موثوقة لبعض خصائص المكمن الأساسية. يمكن لقياسات جس الآبار أن تحدد أو على الأقل تستنتج هذه الخواص: المقاومية، المسامية، حجم السجيل، الصخارية، التشبع المائي، التشبع الهيدروكاربوني والنفاذية. تمثل الدراسة الحالية تقييم للخصائص البتروفيزيائية لآبار فيحاء-1، فيحاء-2 وفيحاء-3 في حقل الفيحاء النفطي وفي بئر سندباد-2 في حقل السندباد النفطي، جنوب العراق. لقد أعتمد التقييم البتروفيزيائي على بيانات مجسات الآبار لتوضيح الخصائص المكمنية لتكويني المشرف واليمامة. إن المجسات البئرية المتوفرة مثل (أشعة كاما، الجهد الذاتي، المقاومة النوعية، مجس المقاومة الدقيق، مجس المقاومة بالحث، الصوتي، الكثافة والمجس النيوتروني) تم تحويلها الى قيم رقمية باستخدام برنامج (Didger v.4). لقد أجريت التصحيحات البيئية والمعاملات البتروفيزيائية مثل المسامية، التشبع المائي، التشبع الهيدروكاربوني وحجم السجيل بأستخدام برنامج البتروفيزياء التفاعلي (IP). تم تحديد الخصائص البتروفيزيائية ورسمها على شكل تفسير المعالجة الحاسوبية (CPI) بأستخدام برنامج (IP). أظهرت الدراسة الصخارية لتكوين المشرف أنه يتكون بشكل رئيسي من تطبقات الحجر الجيري، الدولومايت والسجيل، بينما الدراسة الصخارية لتكوين اليمامة أظهرت أنه يتكون من تطبقات الحجر الجيري، الدولومايت والسجيل في بعض الأعماق.

تفسيرات المجسات البئرية لتكوين المشرف في بئر السندباد-1 أظهرت أنه يمتلك تشبع هيدروكربوني جيد. أشارت النتائج أيضًا إلى أن التشبع الهيدروكاربوني والنفاذية في بعض مديات التكوين وخاصة في وحدة MB عالية جدًا، بالإضافة إلى قلة النفط المتحرك وهذا قد يدل على وجود النفط الثقيل في التكوين. بينما تفسيرات المجسات البئرية لتكوين اليمامة في بئر فيحاء-1 تشير إلى أزدياد التشبع الهيدروكاربوني. بشكل عام، تكون الخصائص المكمنية لتكوين اليمامة في بئر فيحاء-1 أفضل من آبار فيحاء-2 وسندباد-2، والخصائص المكمنية لتكوين المشرف في بئر سندباد-2 أفضل من آبار فيحاء-1 وفيحاء-3 أعتماداً على الخصائص البتروفيزيائية والتشبع النفطي. تم تقسيم تكوين المشرف إلى تسع أنطقة في حقل الفيحاء النفطي وإلى تسع أنطقة في حقل السندباد النفطي، بينما تم تقسيم تكوين اليمامة إلى ست أنطقة في حقل الفيحاء النفطي وسبع أنطقة في حقل السندباد النفطي أعتماداً على سلوك المجسات والحجم السجيلي.

الكلمات المفتاحية: الخواص البتروفيزيائية، تكوين المشرف، تكوين اليمامة، جنوب العراق، المجسات البئرية.